

Department of Electrical Engineering and Automation

Visual Performance Under Mesopic Conditions: Towards Determination of Adaptation Luminance

Can Cengiz



Visual Performance Under Mesopic Conditions: Towards Determination of Adaptation Luminance

Can Cengiz

A doctoral dissertation completed for the degree of Doctor of Science (Technology) to be defended, with the permission of the Aalto University School of Electrical Engineering, at a public examination held at the lecture hall S1 of the school on 13 November 2015 at 12.

Aalto University
School of Electrical Engineering
Department of Electrical Engineering and Automation
Lighting Unit

Supervising professor

Prof. Liisa Halonen

Thesis advisor

Dr. Marjukka Puolakka

Preliminary examiners

Prof. Stephan Völker, Technische Universität Berlin, Germany

Prof. Miyoshi Ayama, Utsunomiya University, Japan

Opponent

Prof. Frangiskos Topalis, National Technical University of Athens, Greece

Aalto University publication series

DOCTORAL DISSERTATIONS 163/2015

© Can Cengiz

ISBN 978-952-60-6439-0 (printed)

ISBN 978-952-60-6440-6 (pdf)

ISSN-L 1799-4934

ISSN 1799-4934 (printed)

ISSN 1799-4942 (pdf)

<http://urn.fi/URN:ISBN:978-952-60-6440-6>

Unigrafia Oy

Helsinki 2015

Finland



Author

Can Cengiz

Name of the doctoral dissertation

Visual Performance Under Mesopic Conditions: Towards Determination of Adaptation Luminance

Publisher School of Electrical Engineering**Unit** Department of Electrical Engineering and Automation**Series** Aalto University publication series DOCTORAL DISSERTATIONS 163/2015**Field of research** Illumination Engineering**Manuscript submitted** 30 April 2015**Date of the defence** 13 November 2015**Permission to publish granted (date)** 22 July 2015**Language** English **Monograph** **Article dissertation (summary + original articles)****Abstract**

The Commission Internationale de l'Eclairage (CIE) published a system for visual performance-based mesopic photometry in 2010. It is valid between the luminances 0.005 cd/m^2 and 5 cd/m^2 . In night-time driving conditions, the luminances in the visual scene are in the mesopic range; thus, mesopic photometry should be adopted when assessing lighting in outdoor areas and other night-time traffic environments. In order to implement the CIE mesopic photometry, the background photopic luminance, i.e. adaptation luminance, is required as an input value.

The aim of the study is to develop methods for estimating the field of view of which the luminance is to be used as the adaptation luminance in implementing the CIE 191 system for mesopic photometry. This is realised by applying methods such as combining eye-tracking data with corresponding luminance data and analysing peripheral target detection under uniform and non-uniform luminous backgrounds.

In the study of combining eye-tracking measurements with luminance data, the visual scene areas with the highest density of gaze distributions were determined. The measured luminances for these visual scenes were used to form an estimate of the adaptation luminance under different driving conditions in the lit and the unlit sections of a rural road. The mean luminances of the estimated fields were higher in the unlit section than in the lit section of the route for all drivers. This was due to high-beam headlights that illuminated the road surface, whereas the gaze points were concentrated in the unlit section.

Experiments in laboratory conditions were conducted in order to obtain the effect of background and target location and its luminance on visual performance. Reaction time and contrast threshold measurements were made to analyse peripheral target detection in uniform and non-uniform backgrounds. Under non-uniform background luminances, peripheral target detection depends on the local luminance of the target and the luminance uniformity of the surrounding area of the target. The results verify that each part of the retina adjusts its sensitivity independently, which refers to local adaptation. However, the complexity of the visual field also has an effect on visual sensitivity in peripheral vision.

Further studies, where road type, driving speed and discomforting glare are taken into account, are needed to define the visual adaptation field and corresponding adaptation luminance in various driving conditions.

Keywords mesopic vision, visual adaptation, eye-tracking, reaction time, contrast threshold**ISBN (printed)** 978-952-60-6439-0**ISBN (pdf)** 978-952-60-6440-6**ISSN-L** 1799-4934**ISSN (printed)** 1799-4934**ISSN (pdf)** 1799-4942**Location of publisher** Helsinki**Location of printing** Helsinki**Year** 2015**Pages** 133**urn** <http://urn.fi/URN:ISBN:978-952-60-6440-6>

Preface

This research work in this thesis was conducted at the Lighting Unit, Aalto University School of Electrical Engineering. The work was supported by Academy of Finland (MAMLI project) and Aalto Energy Efficiency research programme (project Light Energy – Efficient and Safe Traffic Environments).

I am grateful to my supervisor Professor Liisa Halonen for all of her support and encouragement throughout the years that I have been working at the Lighting Unit.

I am also very grateful to my instructor Dr. Marjukka Puolakka for her patient help, critical comments, advice, guidance and priceless contributions during the production of this work.

I would like to thank the preliminary examiners Professor Stephan Völker and Professor Miyoshi Ayama for their valuable comments to improve this thesis. I would also like to thank Professor Frangiskos Topalis for his acceptance to be my opponent in the defense.

I am grateful to M.Sc. Esko Aalto for his priceless contribution in designing and building the experimental setup for laboratory measurements and his great support at all steps of the laboratory experiments. I would like to thank M.Sc. Mikko Maksimainen for useful discussions and his help during the laboratory measurements and contribution in publications V and VI. I am also very grateful to Dr. Mikko Hyvärinen for giving his time and help when needed. I would also like to thank Dr. Anne-Mari Ylinen for her help during road lighting measurements.

I would like to thank Henri Kotkanen, Dr. Esko Lehtonen, Dr. Otto Lappi and Professor Heikki Summala for their extremely valuable contribution in publication II.

I would also like to thank all of my colleagues at the Lighting Unit for the positive working atmosphere.

Finally, my deepest and warmest thanks go to my parents Sevil and Dincer Cengiz, my sister Sevcan and my close friends in Finland for their love, care and support.

Espoo, September 2015
Can Cengiz

List of Publications

This doctoral dissertation consists of a summary and of the following publications that are referred to in the text by their numerals:

- I. Puolakka, Marjukka; Cengiz, Can; Luo, Wei; Halonen Liisa. 'Implementation of CIE 191 Mesopic Photometry – Ongoing and Future Actions'. Proceedings of CIE Lighting Quality & Energy Efficiency, 2012, Hangzhou, September 24–26, p. 64–70.
- II. Cengiz, Can; Kotkanen, Henri; Puolakka, Marjukka; Lappi, Otto; Lehtonen, Esko; Halonen, Liisa; Summala, Heikki. 'Combined eye-tracking and luminance measurements when driving on a rural road: towards determining mesopic adaptation luminance when driving'. SAGE Journals. Lighting Research and Technology, 2014, volume 46, issue 4, pp. 676–694. DOI: 10.1177/1477153513503361.
- III. Cengiz, Can; Puolakka, Marjukka; Halonen, Liisa. 'Reaction time measurements under mesopic light levels'. Proceedings of CIE Lighting Quality & Energy Efficiency, Kuala Lumpur, April 24–26, 2014, pp. 532–537.
- IV. Cengiz, Can; Puolakka, Marjukka; Halonen, Liisa. 'Reaction time measurements under mesopic light levels: Towards estimation of the visual adaptation field'. Accepted for publication in the journal Lighting Research and Technology in the year 2014. Published online before print October 20, 2014. DOI: 10.1177/1477153514554494
- V. Cengiz, Can; Maksimainen, Mikko; Puolakka, Marjukka; Halonen, Liisa. 'Contrast threshold measurements of peripheral targets in night-time driving images'. Accepted for publication in the journal Lighting Research and Technology in the year 2015. Published online before print March 26, 2015. DOI: 10.1177/1477153515578308
- VI. Cengiz, Can; Maksimainen, Mikko; Puolakka, Marjukka; Halonen, Liisa. 'Effects of high luminance objects on peripheral target detection in night-time driving images'. Submitted to the journal Light and Engineering on 18 December 2014.

The author has played a major role at all stages of the work presented in this thesis. The author was responsible for five of the above publications as the main author. In publications III, IV, V and VI, the author collected the information, conducted the experiments and analysed the data. In publication II, the author helped conduct the experiments and analyse the data. In addition, the author was responsible for one publication as a co-author (publication I). The author was responsible for collecting information related to visual adaptation and eye movement measurements.

Contents

Abstract.....	3
Preface.....	5
List of Publications.....	7
Contents.....	9
List of Abbreviations and Symbols.....	11
1. Introduction.....	13
1.1 Background.....	13
1.2 The aim of the study.....	14
2. State of the art.....	15
2.1 Mesopic photometry.....	15
2.2 Adaptation mechanisms of the eye.....	15
2.3 Adaptation in driving conditions.....	16
3. Eye-tracking studies.....	18
3.1 Introduction.....	18
3.2 Field experiments.....	18
3.2.1 Background.....	18
3.2.2 Experimental settings.....	19
3.2.3 Results.....	19
3.2.4 Conclusions.....	24
4. Visual performance experiments.....	25
4.1 Experimental set-up.....	25
4.2 Reaction time measurements under uniform and non-uniform background luminances.....	26
4.2.1 Experimental set-up.....	26
4.2.2 Results.....	29
4.2.3 Discussion.....	33

4.3	Contrast threshold measurements in high-dynamic background images	35
4.3.1	Results	37
4.3.2	The effect of high luminance objects on peripheral target detection	41
4.3.3	Discussion.....	43
5.	Conclusions	46
6.	References	48
7.	Appendices	51

List of Abbreviations and Symbols

Abbreviations

2D	two-dimensional
ANOVA	analysis of variance
CIE	Commission Internationale de l'Eclairage
CT	contrast threshold
IES	Illuminating Engineering Society
KDE	Kernell density estimation
RT	reaction time
SPD	spectral power distribution

Symbols

C	contrast
L_{ave}	average road surface luminance [cd/m^2]
L_b	background luminance [cd/m^2]
$L_e(\lambda)$	spectral radiance [$W \cdot m^{-2} \cdot sr^{-1} \cdot nm^{-1}$]
L_{mes}	mesopic luminance [cd/m^2]
L_t	target luminance [cd/m^2]
S/P ratio	ratio of scotopic to photopic luminous output
TI	threshold increment [%]
U_1	longitudinal luminance uniformity

U_o	overall luminance uniformity
$V(\lambda)$	CIE photopic spectral luminous efficiency function
$V'(\lambda)$	CIE scotopic spectral luminous efficiency function
$V_{mes}(\lambda)$	mesopic spectral luminous efficiency function

1. Introduction

1.1 Background

The basis of all lighting technology and practice lies in photometry, the measurement of visible light. Photometry provides a method with which to assess light in terms of human visual spectral sensitivity. The mesopic luminance region covers a range of luminances between the scotopic and photopic regions. Mesopic lighting applications include road and street lighting, outdoor area lighting and other night-time traffic environments. In the mesopic region the spectral sensitivity of the human visual system is not constant and changes with light level. This is due to the changing contribution of the rods and cones on the retina. Thus, not only one mesopic spectral sensitivity function is needed but instead several functions are needed, together with a defined procedure for using these functions in a photometric measurement system [1].

In 2010, the Commission Internationale de l'Eclairage (CIE) published a system for visual performance-based mesopic photometry [2], which is valid between the luminances 0.005 cd/m^2 and 5 cd/m^2 . In night-time driving conditions, the luminances in the visual scene are in the mesopic range; thus, mesopic photometry should be adopted when assessing lighting in outdoor areas and other night-time traffic environments.

The recommended system for visual performance-based mesopic photometry describes spectral luminous efficiency, $V_{\text{mes}}(\lambda)$, in the mesopic region as a linear combination of the photopic spectral luminous efficiency function, $V(\lambda)$, and the scotopic spectral luminous efficiency function, $V'(\lambda)$, and establishes a gradual transition between these two functions throughout the mesopic region [2]. The system is of the form:

$$M(m)V_{\text{mes}}(\lambda) = mV(\lambda) + (1 - m)V'(\lambda) \text{ for } 0 \leq m \leq 1 \quad (1)$$

and

$$L_{\text{mes}} = \frac{683}{V_{\text{mes}}(\lambda_0)} \int V_{\text{mes}}(\lambda) L_e(\lambda) d\lambda \quad (2)$$

where:

- m is a coefficient, the value of which depends on the visual adaptation conditions;
- $M(m)$ is a normalizing function so that $V_{\text{mes}}(\lambda)$ attains a maximum value of 1;
- $V_{\text{mes}}(\lambda_0)$ is the value of $V_{\text{mes}}(\lambda)$ at 555 nm;
- L_{mes} is the mesopic luminance; and
- $L_e(\lambda)$ is spectral radiance [$\text{W}\cdot\text{m}^{-2}\cdot\text{sr}^{-1}\cdot\text{nm}^{-1}$].

In order to implement CIE mesopic photometry (i.e. calculate mesopic luminance values), the background photopic luminance (i.e. the adaptation luminance) is required as an input value. Also, the ratio of scotopic to photopic luminous output (the S/P ratio) – this is the ratio of the luminous output of a light source evaluated according to the CIE scotopic spectral luminous efficiency function, $V'(\lambda)$, to the luminous output evaluated according to the CIE photopic spectral luminous efficiency function, $V(\lambda)$ – is needed, accounting for the spectral power distribution (SPD) of the light source.

The spectral sensitivity curves underlying CIE mesopic photometry (as well as photopic photometry) were established in constant and uniform adaptation conditions. However, in dynamic outdoor environments the viewing and lighting conditions change constantly. Consequently, the adaptation luminance and hence the spectral sensitivity of vision are subject to change. The next step towards the implementation of mesopic photometry is the definition of adaptation luminance for varied night-time traffic conditions [1].

1.2 The aim of the study

The aim of the study is to develop methods for estimating the field of view, the luminance of which is to be used as the adaptation luminance in implementing the CIE 191 system for mesopic photometry [2]. This is realised by applying methods such as combining eye-tracking and corresponding luminance data, and analysing peripheral target detection under uniform and non-uniform luminous backgrounds.

2. State of the art

2.1 Mesopic photometry

The mesopic luminance region lies between the photopic and scotopic regions where both cones and rods contribute to vision [2, 3]. Unlike the photopic and scotopic spectral luminous efficiency functions, it is not possible to describe mesopic spectral luminous efficiency with a single function since the interaction between cones and rods differs with light levels.

Mesopic vision has many complexities and there have been several models established for mesopic photometry. The earlier models were based on brightness matching, where subjects are asked to match the brightness of a test light with the one in the reference field [4, 5]. However, additivity – in which spectral radiant quantity can be weighted with an appropriate spectral luminous efficiency function and summed linearly across the all wavelengths to quantify corresponding luminous quantity – is not preserved in brightness matching [2]. This is also supported by the fact that target detection and recognition while driving a car are more important than matching the brightness of adjacent surfaces on the road [2]. A recommended system for mesopic photometry based on visual performance was introduced by CIE in 2010 [2]. In this system, the upper limit for mesopic luminance is 5 cd/m^2 and the lower limit is 0.005 cd/m^2 .

Adaptation luminance includes not only the luminance of the foveal field but also that of the peripheral visual field, since both rods and cones contribute to mesopic vision. In some cases it is assumed that adaptation luminance is the average luminance of the whole visual field, but this must be considered a coarse assumption.

2.2 Adaptation mechanisms of the eye

The visual system must adjust its sensitivity to match the ambient light level. This effect is called adaptation [6]. Adaptation is defined as a “process by which the state of the visual system is modified by previous and present exposure to stimuli that may have various luminance values, spectral distributions and angular subtenses” [7]. The adaptation process includes changes in pupil size, neural adaptation and photochemical adaptation. Changes in pupil size occur via the iris, which constricts or dilates in response to an increased or decreased level of retinal illumination [3].

Neural adaptation produced by synaptic interactions in the retina creates a fast change in visual sensitivity (in less than 200 ms) [3]. Photochemical adaptation includes pigment bleaching and regeneration. In the retina, there are four photoreceptors which contain four different pigments. The pigments break down into an unstable aldehyde of vitamin A and a protein (opsin) when light is absorbed [3]. This process is called pigment bleaching. In the dark, the reverse process takes place in the retina. When, for example, a light is turned off, bleached pigments are transformed into an unbleached state; this process is called pigment regeneration [8]. After pigment regeneration, the pigment is able to absorb light again. Pigment regeneration is essential for increasing retinal sensitivity during dark adaptation. The sensitivity of the eye depends on the percentage of unbleached pigment. The concentration of the bleached and regenerated photopigments is in equilibrium under steady retinal irradiance. When retinal irradiance is changed, equilibrium is re-established with pigment bleaching or regeneration. The adaptation duration depends on the magnitude of change in light levels. If the change in retinal illumination is about 2–3 log units, neural adaptation is sufficient. Adaptation is completed in less than one second in this case. For larger changes, photochemical adaptation is necessary. The adaptation process is completed in a few minutes if the change in light level is within the range of operation of the cones. Tens of minutes may be necessary for the completion of the adaptation process if the change is from the operation of the cones to operation of the rods [3].

2.3 Adaptation in driving conditions

In order to implement the CIE 191 mesopic photometric system, the coefficient 'm' needs to be known. It is determined by adaptation luminance. The field of view which contributes to adaptation luminance is called the 'visual adaptation field' [9]. Once it is defined in terms of its size and shape, determining $V_{mes}(\lambda)$ for any scene is possible.

It is also expected that the visual adaptation field is dependent on the behaviour of the person (driving/walking) and also on environmental and illumination conditions. The visual task load is different for example in urban and non-urban traffic routes, and this is expected to affect the relevant visual adaptation field. The gaze of a pedestrian can be assumed to be fixated more often off the road than the gaze of a driver at high driving speeds. Further, the driving speed is expected to affect the eye-fixation area, the area becoming larger with decreased speed.

Driving includes a non-uniform scene with several objects with different lighting intensities. It also includes glare sources that make perception more difficult. Equivalent veiling luminance is defined as 'luminance that, when added by superposition to the luminance of both the adapting background and the object, makes the luminance threshold or the luminance difference threshold the same under the two following conditions: glare present but no additional luminance; additional luminance present but no glare' [7]. Narisada [10] states that when an observer looks at an object against an area in a non-uniform field, the observer's fovea initially adapts to a time average of the luminances of parts of the non-uniform field over which the observer is scanning his or her major visual

attention for a span of time. The initial foveal adaptation luminance to a non-uniform field is increased by the equivalent veiling luminance superimposed. The equivalent veiling luminance rapidly changes with the changes in the observers' gaze points in the non-uniform field.

In driving conditions, drivers are under the effects of continuous illumination changes that require rapid adaptation processes in some cases, such as when driving from a well-lit tunnel to an unlit road area [11]. In such a case it will take some time to reach the maximal visual sensitivity and adapt to the illumination change.

Although foveal vision is important in driving, peripheral visual information is also critical – it is needed in detecting traffic signs, pedestrians, cyclists and other vehicles on the road [11, 12]. However, it should be noted that visual sensitivity decreases in the peripheral retina [12].

According to Alferdinck et al. [13] a new adaptation model can be defined by combining the local adaptation luminances (the 'average luminance of a 2 degree spot in the centre of the scene' [13]) and global adaptation luminances (the 'average luminance of the whole scene perceived by the observer' [13]), and by considering eye movements. To consider the local adaptation luminance the global adaptation luminance may cause overestimation if the road user is looking at a local spot with low luminance, such as the road surface. On the other hand, there can be underestimation if the observer has gazed at a highly lit advertisement beside the road. Moreover, adaptation luminance will be underestimated if it is set to the global adaptation luminance due to the disability glare, as mentioned previously. The adaptation luminance depends on eye movements and luminous distribution of the visual field in various traffic environments [13].

3. Eye-tracking studies

3.1 Introduction

Eye-tracking is a method of measuring gaze points and eye movements. It is possible to measure gaze directions, pursuit movements and fixation duration with an eye-tracker. In defining the visual adaptation field one question is 'Where do drivers look while driving?' Measurement and analysis of eye-movements in night-time driving is one way to answer this question.

Eye-movement behaviour is affected by several factors, such as driving experience, age, road and traffic type, and lighting conditions [14, 15, 16]. When driving, there are several objects visible through the windscreen of the car and in the mirrors. The luminance values of the stimuli and their surroundings are not constant while driving but change dynamically. The use of an eye-tracker presents foveal eye fixation and does not give any information about peripheral vision. However, it is useful for obtaining data for the area that is scanned by drivers' eyes under night-time driving conditions.

The sampling behaviour of the driver's gaze, moreover, determines the illuminance distribution at different parts of the retina over time. The driver samples the road scene, the mirrors and the car's interior by performing saccadic eye movements interspersed with fixations or pursuit movements, which bring specific objects or locations into high-resolution foveal vision [17–21].

3.2 Field experiments

3.2.1 Background

In this work, field experiments were conducted in co-operation with the Helsinki University Traffic Research Unit to measure the eye-behaviour of drivers while driving at day and night. Along with the eye-fixation measurements the luminance distributions of the driving scenes were measured.

The aim was to determine the extent of the visual scene that drivers spend most of their time looking at and to combine this information with the luminance measurements. The luminance values are expected to vary according to various parameters, such as road characteristics, driving speed, the type of road lighting and the surrounding lighting. In this study, fields of view with circular sizes of 1° , 5° , 10° , 15° and 20° around the peak gaze distributions were analysed as the initial estimates of the extent of the visual fields that govern the adaptation state of the eye.

3.2.2 Experimental settings

Three drivers (mean age: 25) were asked to drive on a rural road in Helsinki both in the daytime and at night-time. The car was equipped with two-camera Smart Eye Pro 5.5 eye-trackers operating at 60 Hz and with a luminance camera (Opte-e-ma LMK98-3 Colour). Eye-behaviours and corresponding luminance values were recorded in lit sections (5.0 km) and unlit sections (6.5 km) of the road.

The road was illuminated by high-pressure sodium lamps; the lighting installation was built in 1995 and the lighting design was made for the lighting class AL4a [22] (average road surface luminance $L_{ave} = 1.0 \text{ cd/m}^2$; overall luminance uniformity, $U_o = 0.4$; longitudinal luminance uniformity $U_l = 0.4$; threshold increment $TI = 15\%$).

The lit and unlit sections were divided into 25-m bins along the road in order to obtain accurate data due to the difficulties in synchronizing the eye-tracking and the luminance cameras. For each 25-m bin, a median luminance image was computed from all the luminance images captured during that particular road bin (number of luminance images captured during a 25-m bin: mean ± 16.2 ; standard deviation ± 2.1). In the analyses, these aggregate median luminance images were considered to represent the road scene and its luminance distribution during the respective 25-m long segments.

3.2.3 Results

A two-dimensional (2D) histogram of the distribution of the gaze direction for each road bin was calculated separately for the daylight and night-time driving sessions of each participant. Such a histogram describes the distribution of the measured gaze directions relative to the centre line of the vehicle. The resulting histograms were smoothed with a Gaussian kernel to calculate the contours. Based on the 2D histogram, it is possible to calculate the mode of the gaze distributions and the different levels of the contours.

The gaze distributions in the horizontal direction were almost the same in the lit section of the road both in daytime and night-time conditions. The locations (vertical declination and horizontal eccentricity) of the peaks of the gaze distribution in the road bins, averaged for each of the subjects, are presented in Figures 1 and 2. To describe the spread of the gaze, 50% contour levels (50% of the gaze observations are within the contour) were calculated. The extent of the contours in the horizontal and vertical directions is shown in Figure 3.

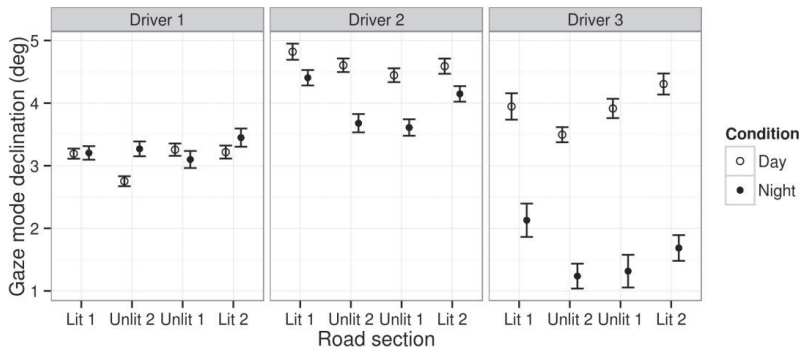


Figure 1. Vertical declination of the gaze concentration mode, averaged over the road bins separately for each road section, condition (day/night) and subject. The origin is at the principal point of the image, which is approximately at the level of the horizon. The error bars represent a 95% confidence level.

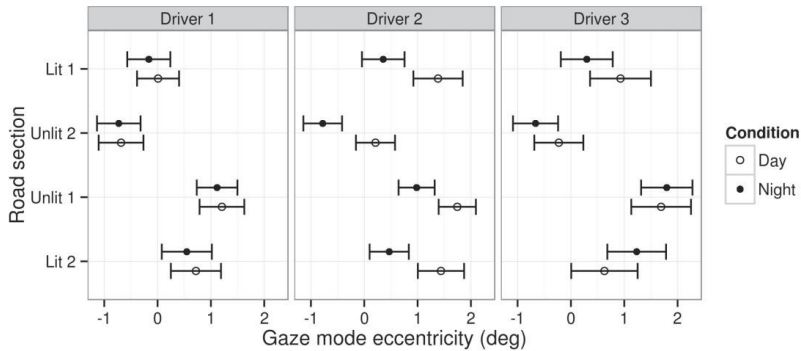


Figure 2. Horizontal eccentricity of the gaze concentration peak, averaged over the road bins separately for each road section, condition (day/night) and subject. Negative values indicate that the driver's gaze has fallen to the left of the vehicle's centre line. The error bars represent a 95% confidence level.

Compared to the daylight conditions, drivers 2 and 3 directed their gaze more downwards during the night, as can be seen in Figure 1. For those drivers, there seemed to be a shift in their gaze behaviour, which could be due to the difficulty of viewing beyond the area illuminated by the car's headlights, especially in unlit road conditions.

The horizontal mode of the gaze distribution of the subjects remained close to the vehicle's centre line in the lit sections at night (Figure 2). In the unlit sections at night all drivers' gaze modes were to the right of the centre line in section 1 (northbound) and mostly to the left in section 2 (southbound). However, as this effect was present both in daytime and night-time conditions it is attributable to the geometry of the road.

The size of the 50% contour of the gaze distributions was consistently larger in the vertical dimension during the night, while the horizontal dispersion remained approximately the same between daytime and night-time conditions, as seen in Figure 3. This suggests that in the night-time conditions, drivers move their gaze more vertically, scanning the road near and far. The vertical range of the 50% contour was markedly larger for drivers 2 and 3, whose vertical declination of the mode was also lower during night-time conditions compared to daytime conditions (Figure 1). The gaze behaviours of driver 1, who was the most experienced driver, was approximately the same in both conditions; likewise, the vertical range of the 50% contour during night-time conditions was closer to the daytime range. This effect is also visible in Figure 4 which indicates the contours of the gaze distributions for all daytime and night-time data in the lit section.

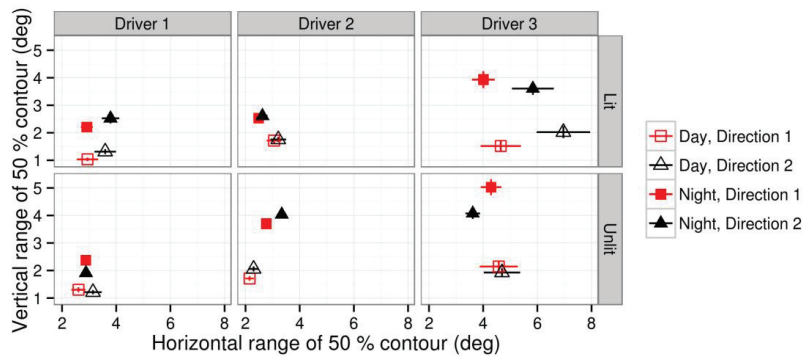


Figure 3. Dispersion of the gaze, averaged over the road bins separately for each road section, condition (day/night) and subject. The error bars represent a 95% confidence level.

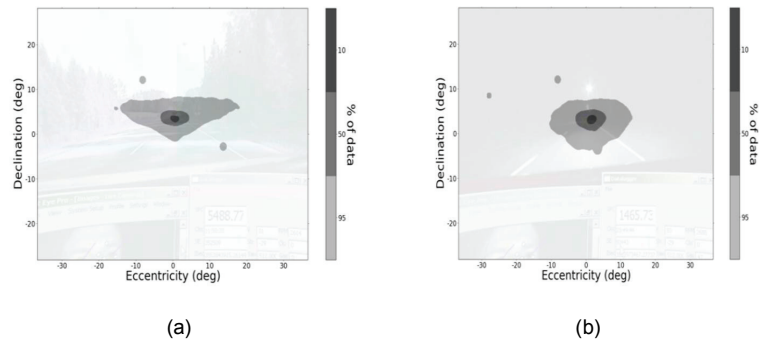


Figure 4. (a) Contours of the gaze distribution (10%, 50% and 95% contours from the innermost to the outermost contours, respectively) superimposed on a video image of daytime driving in the lit section. (b) Contours of the gaze distribution (10%, 50% and 95% contours from the innermost to the outermost contours, respectively) superimposed on a video image of night-time driving in the lit section.

Median luminance images for each 25-m bin (Figure 5) were calculated for the night-time conditions. These images represent the view of the road visible to the driver during a 25-m stretch of the road.

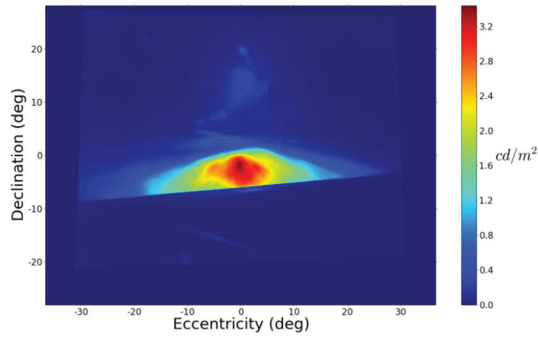
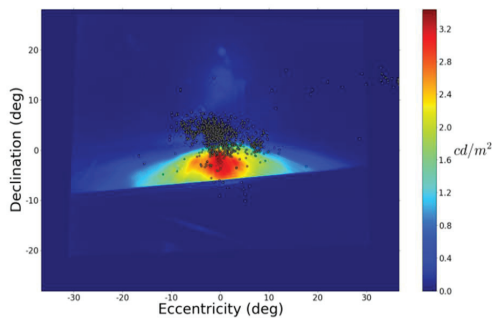
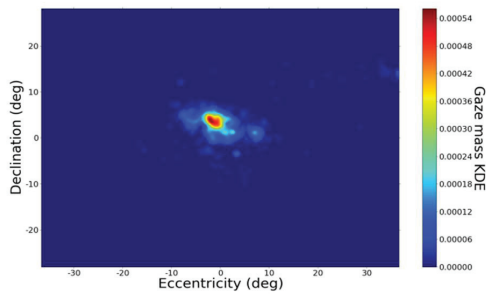


Figure 5. An example of a median luminance image, computed from all the luminance images captured in the lit section within a 25-m bin.

It should be noted that the underlying image in Figures 5, 6a and 8 is the same, the colour scale that can be seen in Figure 5. The eye-tracker reveals only the foveal fixations, shown in Figure 6a. The gaze density computed using a 2D histogram is indicated in the form of a heat map in Figure 6b.



(a)



(b)

Figure 6. Median luminance images from a 25-m bin on a lit segment (the gaze data on both images are the same: all luminance data for each driver and each run from inside the 25-m bin was aggregated): (a) scatter of the gaze data points; (b) gaze density estimate, indicated as a heat map with gaze mass density estimation (kernel density estimation – KDE) computed from the histogram.

The gaze distributions within the scene are illustrated as contour lines (Figure 7). The mean luminances were calculated for the area within the different fields of view, defined as circular 1° , 5° , 10° , 15° and 20° fields (Figure 8) that have their centre at the peak of the gaze distributions (Figure 6b) for each 25-m bin. Those areas represent the initial estimates for the visual adaptation field. The upper limit of the fields was 20° . Above the 20° field, we would probably have observed the same luminance values without any eye-behaviour related effects, since the visual field would in that case cover most of the windscreen.

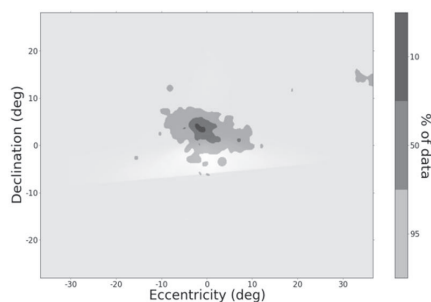


Figure 7. Contours of the gaze distribution (10%, 50% and 95% contours from the innermost to the outermost contours, respectively) superimposed on a median luminance image (pictured: observations of all drivers during a 25-m bin on the lit route at night-time).

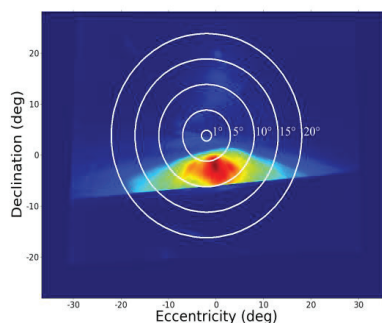


Figure 8. The circular 1° , 5° , 10° , 15° and 20° fields imposed to the median luminance image (Figure 5) as an initial estimation of the visual field. The centre point of the circular fields is the peak (mode) of the histogram, from which the contours in Figure 6a are also derived.

The mean luminances were calculated for circular fields of 1° , 5° , 10° , 15° and 20° centred at the peak of the gaze distribution. This was done both for the lit and unlit conditions (Tables 1 and 2).

On the unlit section of the road the drivers looked more downwards, since there was only illumination from the car headlights on the road surface close to the car. Therefore, higher luminance values were obtained in the unlit section relative to the lit section (Table 2). The differences in the circular field luminances between the subjects become smaller with increased circular field sizes.

Table 1. The mean luminance values for the 1°, 5°, 10°, 15° and 20° circular fields, calculated from all of the bins in the lit sections for all of the drivers.

The luminance of the circular visual fields (cd/m ²) mean ± standard deviation						
Drivers	Condi- tion	1° field	5° field	10° field	15° field	20° field
Driver 1	Lit 1	0.43 ± 0.18	0.72 ± 0.21	0.90 ± 0.14	0.63 ± 0.10	0.44 ± 0.08
	Lit 2	0.34 ± 0.25	0.64 ± 0.26	0.84 ± 0.13	0.61 ± 0.07	0.43 ± 0.06
Driver 2	Lit 1	0.27 ± 0.14	0.48 ± 0.20	0.78 ± 0.16	0.61 ± 0.10	0.44 ± 0.08
	Lit 2	0.27 ± 0.13	0.50 ± 0.21	0.80 ± 0.13	0.61 ± 0.07	0.43 ± 0.06
Driver 3	Lit 1	0.85 ± 0.81	1.05 ± 0.52	0.94 ± 0.21	0.63 ± 0.11	0.44 ± 0.09
	Lit 2	0.93 ± 0.72	1.11 ± 0.46	0.93 ± 0.16	0.61 ± 0.09	0.43 ± 0.07

Table 2. The mean luminance values for the 1°, 5°, 10°, 15° and 20° circular fields, calculated from all of the bins in the unlit sections for all of the drivers.

The luminance of the circular visual fields (cd/m ²) mean ± standard deviation						
Drivers	Condi- tion	1° field	5° field	10° field	15° field	20° field
Driver 1	Unlit 1	0.89 ± 1.07	1.83 ± 0.77	1.70 ± 0.20	1.03 ± 0.06	0.65 ± 0.04
	Unlit 2	0.65 ± 0.73	1.67 ± 0.71	1.67 ± 0.21	1.03 ± 0.07	0.65 ± 0.04
Driver 2	Unlit 1	0.51 ± 0.74	1.53 ± 0.66	1.65 ± 0.17	1.02 ± 0.06	0.65 ± 0.04
	Unlit 2	0.52 ± 0.85	1.45 ± 0.72	1.62 ± 0.22	1.03 ± 0.07	0.65 ± 0.04
Driver 3	Unlit 1	3.35 ± 2.68	2.83 ± 1.32	1.76 ± 0.37	1.02 ± 0.10	0.65 ± 0.04
	Unlit 2	3.32 ± 2.46	2.94 ± 1.13	1.85 ± 0.23	1.05 ± 0.08	0.66 ± 0.05

For all circular fields, the mean luminance values for each driver for the entire distance were higher in the unlit sections compared to the lit sections due to the use of high-beam headlights in the unlit section. The mean luminance differences between the three drivers decreased as the circular field size increased. Moreover, the variations in the mean luminance values diminished as the size of the circular visual field increased.

3.2.4 Conclusions

In this study the visual scene areas with the highest density of gaze distributions were determined. The measured luminances for these visual scenes were used to form an estimate of the adaptation luminance under different driving conditions. The estimated fields of view were circular in shape. The mean luminances of the estimated fields were higher in the unlit section than in the lit section of the route for all drivers due to the gaze points on the road surface illuminated by the high-beam headlights in the unlit section. The differences in the mean luminance between three drives decreased as the field size increased. Moreover, the variations in the mean luminance values diminished as the size of the circular visual field increased.

Further studies are needed to study the size and location of the area defining the visual adaptation field and whether its shape can be assumed to be circular, ellipsoid or some other shape. This study assumed that the gaze distributions defined the centre of the field of view. Additional studies are needed to verify whether or not the centre of the visual field is the same as the centre of the visual adaptation field.

4. Visual performance experiments

The visual adaptation field refers to the extent of the field of view that determines the adaptation state of the eye. Therefore, it is important to estimate the extent of the space visible to the eye by analysing peripheral target detection. Conducting experiments in laboratory conditions makes controlling the location and luminance of the target and background possible. Thus, it is expected to get useful data related to visual performance against targets in peripheral vision.

Night-time driving is the most essential field in which mesopic photometry can be applied [2]. Both foveal vision (dominated by cones) and peripheral vision (an interaction of cones and rods) are needed in driving. Peripheral target detection is critical, for example during the sudden appearance of pedestrians, animals and other vehicles in the visual field. The appearance of targets at different eccentricities and with different luminances is a useful method for analysing peripheral visual performance.

4.1 Experimental set-up

A large screen illuminated by three projectors (BenQ W1070) was used to create a background and stimuli for the visual experiments. The size of the visual field provided by the screen was 180° horizontally and 44° vertically. The distance between the subjects and the fixation point was 96 cm (Figure 9).

A Labview programme was developed to adjust the luminance, size and locations of the targets. The duration of target appearance and the type of background in terms of uniformity and spectra were also controlled by the programme. Neutral density filters were applied in the projectors to provide mesopic luminances on the screen.

Reaction time and contrast threshold experiments were conducted by asking the subjects to detect off-axis targets while they were fixated at the cross in the centre of the screen. The fixation location was monitored with an infrared camera located below the screen. An LMK luminance measuring imaging photometer and an LMT L1009 luminance meter were used in luminance measurements. Spectral irradiance measurements were done using a Konica Minolta CL-500 A Illuminance Spectrophotometer.

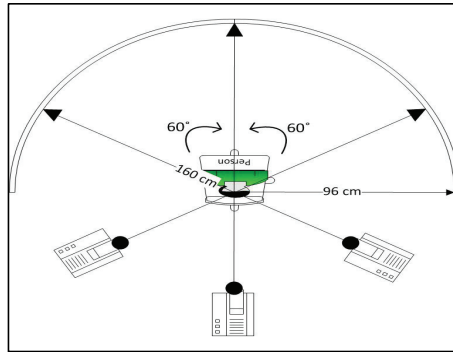


Figure 9. The large screen used in reaction time and contrast threshold experiments.

4.2 Reaction time measurements under uniform and non-uniform background luminances

Reaction times to visual stimuli are strongly related to driving performance and traffic safety [23–24]. A link between the response-time based relative visual performance model and the reduction in crashes for roadway intersections was reported by Rea [23]. Plainis and Murray [24] hypothesised that longer reaction times under dark conditions might be the explanation for the higher crash rates at night-time relative to the daytime.

Driving includes miscellaneous stimuli in various locations. More data are thus needed about visual performance at larger eccentricities for estimating the extent of the visual adaptation field in mesopic conditions. Reaction times to peripheral targets under uniform and non-uniform backgrounds are good indicators for estimation of the extent of the visual field.

4.2.1 Experimental set-up

Reaction times to targets located at eccentricities between -75° and 75° in the horizontal axis and at -15° and 15° in the vertical axis were measured.

The reaction times and numbers of missed targets are expected to contribute to estimating the size and the shape of the visual adaptation field in mesopic conditions. The effects of target eccentricity and contrast, light spectrum and luminance level on peripheral target detection under different adaptation conditions were analysed.

The type of the visual scene background is an essential factor in assessing adaptation conditions at mesopic light levels. Backgrounds with uniform luminance have been used in some studies [25–26]. It is also important to analyse the effects of the non-uniformity of the background luminance on visual performance since the visual scene in driving at night includes various luminances. This has been done in the studies of Uchida et al. and Akashi et al. [9] [27]. Therefore,

the comparison of visual performance under uniform and non-uniform background luminances is expected to provide information for analysing visual adaptation in night-time driving.

Three uniform and three non-uniform background luminances were applied in the experiments. The light spectra for the uniform backgrounds were red, blue and white. The uniformity of the background luminances were analysed by LMK LabSoft. The luminance uniformity was within 10%. The light spectrum for non-uniform backgrounds was white. The spectral distributions are shown in Figure 10. The S/P ratios of the light spectra were 0.3 (red), 2.18 (white) and 12.18 (blue). Achromatic stimuli of a 1.5° size were projected onto the background in 35 different locations (Figure 11). The horizontal target eccentricities were -75° , -45° , -10° , 0° , 10° , 45° and 75° and the vertical target eccentricities were -15° , -7° , 0° , 7° and 15° . The two background luminances of the uniform backgrounds were 0.1 cd/m^2 and 1 cd/m^2 .

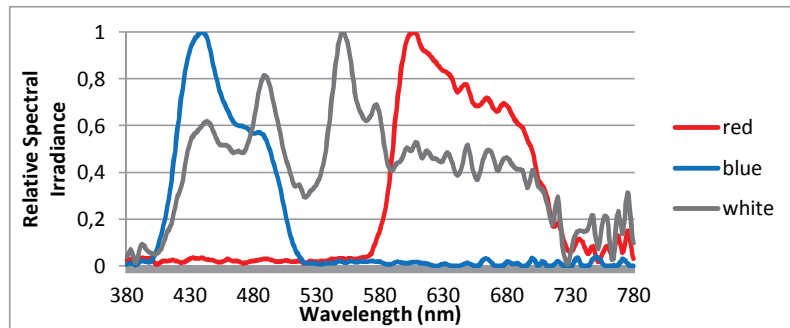


Figure 10. The relative SPDs for red, blue and white light.

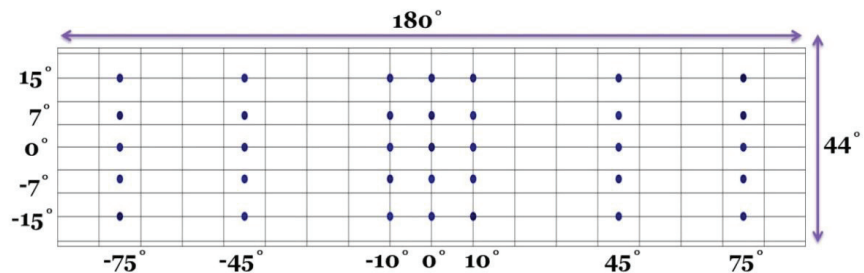


Figure 11. Screen size and target locations in terms of horizontal and vertical eccentricities.

The target contrasts were 0.3 and 0.7 for the uniform backgrounds at a background luminance of 1 cd/m^2 . The target contrast was 0.7 for the uniform backgrounds at a background luminance of 0.1 cd/m^2 and for all non-uniform backgrounds.

For non-uniform backgrounds, three different luminance patterns (elliptical, road scene and windscreen) with a 1 cd/m² luminance were imposed on the uniform background with a 0.1 cd/m² luminance. The patterns in terms of their size and luminance are presented in Figure 12.

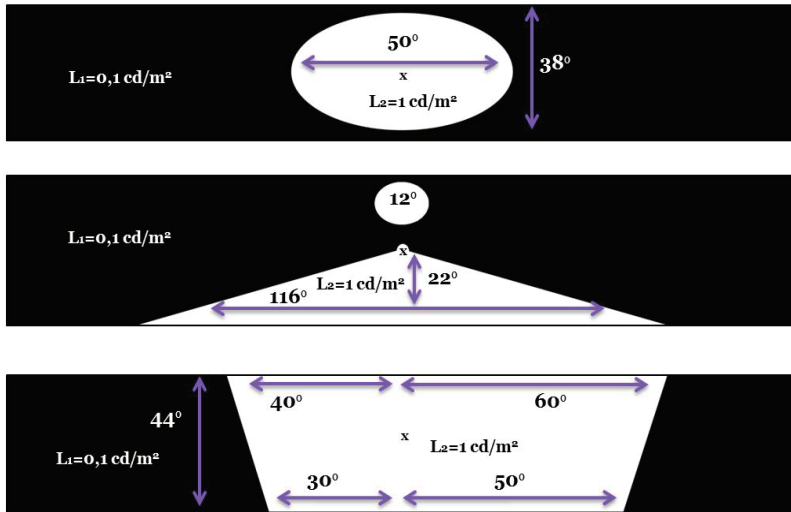


Figure 12. The non-uniform backgrounds applied in the experiment. Three different patterns illustrating elliptical (above), road scene (middle) and windscreen (below) with a luminance of 1 cd/m² imposed on a background with a luminance of 0.1 cd/m². White light was used for all the non-uniform backgrounds.

The contrast was calculated by the equation:

$$C = (L_b - L_t)/L_b \quad (3)$$

where C is the contrast, L_b is the background luminance and L_t is the target luminance.

Ten subjects (five females and five males), with a mean age of 28, participated in the experiment. During the experimental session, the subjects were asked to fixate on the cross at the centre of the screen and press the button when they detected the stimulus. The time between the stimulus appearance and the subject's response was recorded as the reaction time.

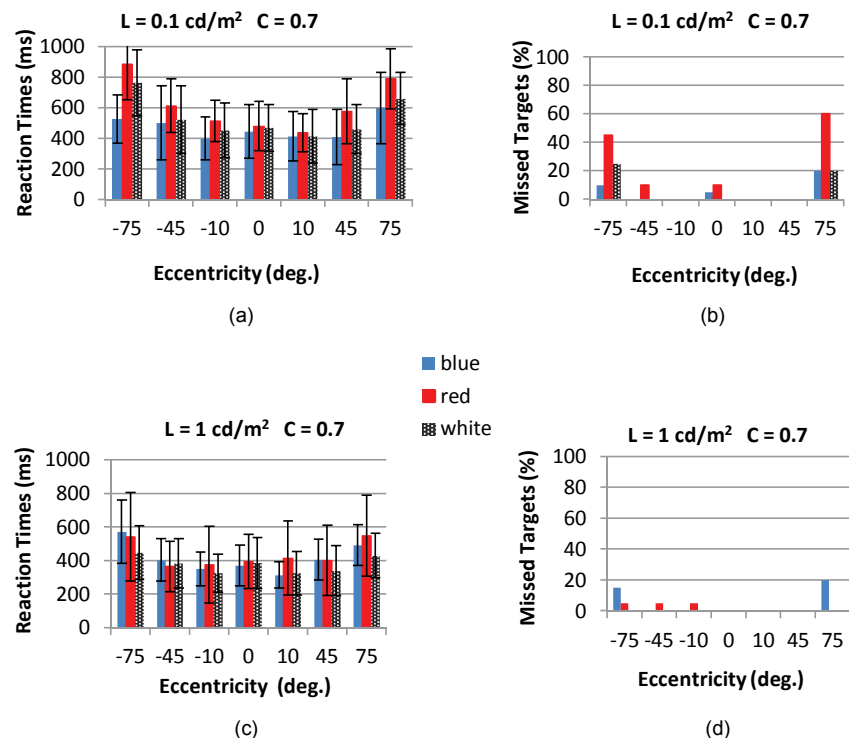
The reaction time values include a delay caused by the software and interconnection of the devices in the system. The mean delay of the system was found to be 290 ms with a standard deviation of 12.6. This delay time was subtracted from the measured reaction time values.

4.2.2 Results

4.2.2.1 Reaction time under uniform background luminances

Mean reaction times for stimuli appearing at horizontal eccentricities of -75° , -45° , -10° , 0° , 10° , 45° and 75° for uniform backgrounds with a luminance of 1 cd/m^2 and 0.1 cd/m^2 are presented in Figure 13. The graphs indicate the target locations on the horizontal axis where vertical eccentricity is zero. The mean reaction times for foveal targets with 0.3 and 0.7 contrasts for blue and white backgrounds were longer than those at the -10° and 10° eccentricities. The mean reaction times to targets with 0.7 contrast appearing in the near periphery (-10° and 10° eccentricities) at 0.1 and 1 cd/m^2 for the red background were higher compared to those for the white and blue backgrounds (Figure 13 a, 13c). Mean reaction times at -75° , 45° and 75° target eccentricities under the white background at 1 cd/m^2 were lower than the red and blue backgrounds for both contrast values (Figures 13c, 13e). The number of missed targets was high for low-contrast targets at the far periphery under blue light.

The effect of the light spectrum on reaction time is evident at a background luminance 0.1 cd/m^2 , as shown in Figure 13a. In foveal vision the light spectrum did not affect the reaction time. However, reaction times to peripheral stimuli under blue light were shorter than those for the white and red light spectra.



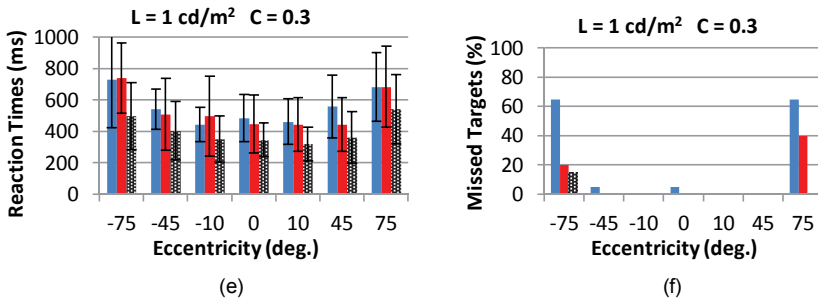


Figure 13. Mean reaction times and the percentage of missed targets as a function of horizontal target eccentricities, light spectrum, background luminance and contrast for uniform backgrounds. The error bars indicate the standard deviation. L = luminance. C = contrast.

Figure 14a shows the effect of contrast on reaction times averaged over all background spectra at 1 cd/m² background luminance. The effect of background luminance on reaction times to stimuli with 0.7 contrast is also shown in Figure 14b.

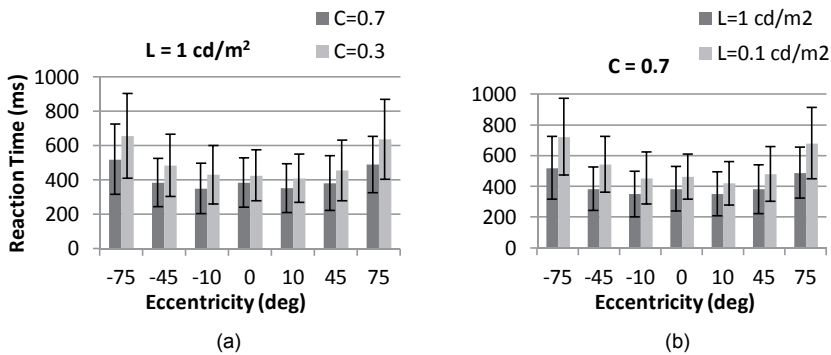


Figure 14. Mean reaction times as a function of horizontal eccentricities for uniform backgrounds, averaged over all light spectra. (a) The effect of contrast on reaction time for a 1 cd/m² luminance. (b) The effect of background luminance on reaction time to stimuli with a 0.7 contrast. The error bars indicate the standard deviation. L = luminance. C = contrast.

The effects of background luminance, light spectrum and target location on reaction time in terms of horizontal and vertical eccentricities were analysed by performing an analysis of variance (ANOVA). The ANOVA includes all light spectra (red, blue and white) and two luminance levels (0.1 and 1 cd/m²). Table 3 shows the results of the ANOVA.

The target location affected visual performance in terms of reaction time under uniform backgrounds at both luminances and with all light spectra. The reaction times and the percentage of missed targets greatly increased at -75° and 75° target eccentricities. The difference in mean reaction times between 75° and 45° target eccentricities was higher than those for other eccentricities.

In order to find out the target location at which the subjects' reaction time started to increase, additional experimental sessions were conducted for two subjects under uniform backgrounds. In these sessions, the furthest peripheral target location was 60° and -60° instead of the 75° and -75° eccentricities. The reaction times to targets at 45° and 60° eccentricities were similar, except for with the low-contrast target under blue light. The percentage of missed targets at 60° eccentricity was significantly lower than those at 75° eccentricity. Reaction times started to increase at the eccentricities larger than 60°. There were no missed targets at 60° eccentricity at a background luminance of 1 cd/m² and for the target contrast of 0.7.

Table 3. Results of statistical analysis (ANOVA) for reaction time and missed targets under uniform backgrounds. The significant differences are indicated in bold.

Source of variation	df	Reaction Time		Missed Targets	
		F	p-values	F	p-values
Horizontal eccentricity	6	183.45	0.00	379.96	0.00
Vertical eccentricity	4	10.67	0.00	33.63	0.00
Luminance	1	774.20	0.00	266.35	0.00
Colour	2	63.38	0.00	44.11	0.00
H. eccentricity x V. eccentricity	24	1.85	0.01	15.93	0.00
H. eccentricity x Luminance	6	13.35	0.00	87.25	0.00
H. eccentricity x Colour	12	0.71	0.74	9.15	0.00
V. eccentricity x Luminance	4	1.07	0.37	0.68	0.61
V. eccentricity x Colour	8	0.65	0.73	1.12	0.35
Luminance x Colour	2	71.93	0.00	146.11	0.00
H. eccentricity x V. eccentricity x Luminance	24	1.38	0.12	1.13	0.31
H. eccentricity x V. eccentricity x Colour	48	1.66	0.01	0.83	0.77
H. eccentricity x Luminance x Colour	12	7.29	0.00	54.57	0.00
V. eccentricity x Luminance x Colour	8	0.92	0.50	5.37	0.00
H. eccentricity x V. eccentricity x Luminance x Colour	48	1.09	0.33	2.69	0.00

4.2.2.2 Reaction times under non-uniform background luminances

The mean reaction times increased with increasing eccentricity for most of the background configurations (Figure 15). For the non-uniform background with the road scene pattern, the mean reaction times for foveal targets were significantly higher than for the other backgrounds. The only missed target recorded at that eccentricity was also recorded in the non-uniform background with the road scene (non-uniform 2). It can be attributed to the shape of the road scene pattern that is more complex than the elliptical and windscreen pattern in non-uniform images (Figure 12).

The results indicate that reaction times to stimuli at the far periphery (-75°, -45°, 45° and 75° eccentricities) depend on the local luminance of the stimulus rather than on the luminance uniformity of the background. In other words, for a stimulus appearing at 45° eccentricity, the stimulus luminance is

0.17 cd/m² for the uniform 1 ($L_b = 0.1$ cd/m²), non-uniform 1 (elliptical) and non-uniform 2 (road scene) backgrounds, whereas it becomes 1.7 cd/m² for the uniform 2 ($L_b = 1$ cd/m²) and non-uniform 3 (windscreen) backgrounds. The mean reaction times to targets appearing at the far periphery and having the same target luminance were similar under different background images. However, luminance distribution of the background affected reaction times to stimuli at -10° , 0° and 10° eccentricities.

The statistical analysis of reaction time and the percentage of missed targets was performed with the ANOVA test (Table 4). Both the horizontal and vertical eccentricities and target luminance affect the mean reaction time and the percentage of missed targets. Although the effect of the background luminance uniformity on reaction time is not significant, it has a significant effect on the percentage of missed targets. A post hoc Bonferroni test was applied to analyse the effect of eccentricity on mean reaction time. This statistical method also indicates that the difference in mean reaction times is significant at -75° , -45° , 45° and 75° target eccentricities.

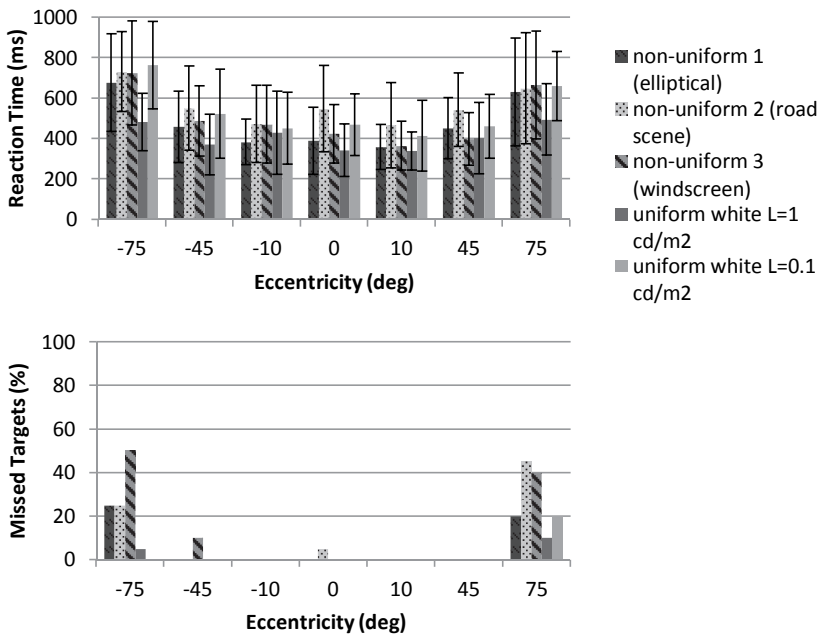


Figure 15. Mean reaction times and the percentage of missed targets as a function of horizontal target eccentricities, for uniform and non-uniform backgrounds. The background spectrum was white. Vertical eccentricity was zero. The immediate background luminances of non-uniform 1 (elliptical) are 1 cd/m² for -10° , 0° , 10° eccentricities; 0.1 cd/m² for -75° , -45° , 45° and 75° eccentricities. For non-uniform 2 (road scene), the immediate background luminances are 1 cd/m² for 0° eccentricity; 0.1 cd/m² for -75° , -45° , -10° , 10° , 45° and 75° eccentricities. For non-uniform 3 (windscreen), immediate background luminances are 1 cd/m² for -10° , 0° , 10° , 45° eccentricities; 0.1 cd/m² for -75° , -45° and 75° eccentricities. The contrast ratio was 0.7. The error bars about mean reaction time indicate the standard deviation.

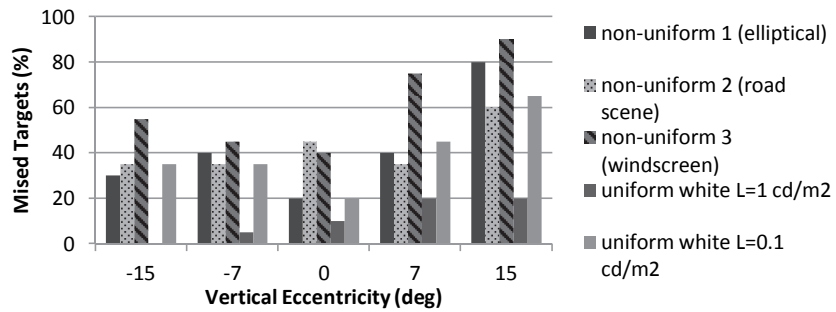


Figure 16. The percentage of missed targets as a function of vertical eccentricities, for uniform and non-uniform backgrounds. Horizontal eccentricity was 75° . The background spectrum is white. The target contrast was 0.7.

The effect of vertical target eccentricity on reaction time is shown in Figure 16, which presents the number of missed targets as a function of vertical eccentricity. In this case, the horizontal eccentricity was 75° , which is the furthest horizontal location. It is seen that the percentage of misses was affected by the background luminance pattern rather than by the local luminance of the target. Local luminance refers to the luminance of the target according to its location and the luminance of its surroundings. The luminance of the target located in the 0.1 cd/m^2 luminance region of the non-uniform background is 0.17 cd/m^2 , whereas it is 1.7 cd/m^2 in the mask of the background image of which luminance is 1 cd/m^2 (Figure 12).

Table 4. The results of statistical analysis (ANOVA) for reaction time and missed targets under non-uniform backgrounds. Significant parameters are indicated in bold.

Source of variation	df	Reaction Time		Missed Targets	
		F	p-values	F	p-values
Horizontal eccentricity	6	72.45	0.00	4103.55	0.00
Vertical eccentricity	4	3.57	0.01	351.40	0.00
Luminance	1	170.67	0.00	275.57	0.00
Uniformity	1	1.30	0.26	1349.38	0.00
H. eccentricity x V. eccentricity	24	1.26	0.18	116.24	0.00
H. eccentricity x Luminance	6	5.61	0.00	481.07	0.00
H. eccentricity x Uniformity	6	3.19	0.00	1075.64	0.00
V. eccentricity x Luminance	4	0.57	0.69	17.10	0.00
V. eccentricity x Uniformity	4	0.55	0.70	29.05	0.00
Luminance x Uniformity	1	0.56	0.46	6.63	0.01
H. eccentricity x V. eccentricity x Luminance	24	0.89	0.62	24.15	0.00
H. eccentricity x V. eccentricity x Uniformity	24	0.89	0.62	31.15	0.00
H. eccentricity x Luminance x Uniformity	6	0.26	0.85	1.87	0.13
V. eccentricity x Luminance x Uniformity	4	1.18	0.32	4.22	0.00
H. eccentricity x V. eccentricity x Luminance x Uniformity	24	0.48	0.75	2.79	0.03

4.2.3 Discussion

The results indicate that the target luminance, location and luminance distribution of the background affect reaction times under mesopic light levels. The target luminance and location have a major effect on both mean reaction times and

the percentage of missed targets. Under both uniform and non-uniform background luminances, the mean reaction times to stimuli in the fovea and close to the fovea (-10° and 10°) are similar. However, in the far periphery the increases in mean reaction time are clearly seen.

The spectral sensitivity changes at mesopic light levels were only observed at the lower background luminance of 0.1 cd/m^2 . At this luminance, the mean reaction time to peripheral stimuli under blue light is shorter than under the other light spectra. However, at the higher background luminance ($L = 1 \text{ cd/m}^2$) and at contrast of 0.7 ($C = 0.7$), the mean reaction time to peripheral stimuli is similar under red and blue light. At this luminance level there were more misses than with the lower contrast of 0.3 ($C = 0.3$) under blue light than under white or red light. These unexpected results could be due to the fact that the level of the subjects' visual comfort was lower in blue background at 1 cd/m^2 relative to the other spectra.

For non-uniform backgrounds, the difference in mean reaction times between target eccentricities 0° and 10° was small, except for with the background representing a road scene. The differences in mean reaction times for foveal stimuli may be due to the luminance distribution of the background. The effect of stimulus location and luminance on mean reaction times was most visible at target eccentricities of -75° , -45° , 45° and 75° . The mean reaction times to stimuli at the far periphery were affected by the local luminance of the stimulus which supports the local adaptation approach that states that each part of the retina adjusts its adaptation level to the local light level independently [9][28-29]. As expected, the percentage of missed targets was higher at eccentricities of 75° and -75° for all backgrounds. The effect of luminance distribution is stronger on the percentage of missed targets under non-uniform backgrounds than under uniform backgrounds. For example, half of the subjects missed the target appearing at -75° with the non-uniform background representing a windscreen, whereas there were no missed targets at the same eccentricity with a uniform background (0.1 cd/m^2) although the target luminances were the same.

The high number of missed targets at -75° and 75° eccentricities for non-uniform backgrounds indicates that the luminance distribution of the background affects visual performance for stimuli appearing in the far periphery. In other words, the detection of targets at -75° and 75° is more difficult under non-uniform background luminances than under uniform background luminances.

The effect of vertical eccentricity on the percentage of missed targets at 75° is shown in Figure 16. For targets at 75° horizontal and 15° vertical eccentricities, the number of missed targets was 90% for the non-uniform background pattern representing a windscreen. This indicates that it was almost impossible to detect targets around the furthest horizontal and vertical eccentricities. The changes in mean reaction time as a function of vertical eccentricity at 75° horizontal eccentricity indicate that the shape of the functional visual field is elliptical. The

difference between mean reaction times at 60° and 75° horizontal eccentricities under uniform background luminances also supports this observation.

However, by considering targets with different size and contrast and also visual tasks different from reaction time, it is not straightforward to suggest the above-mentioned area as the shape and the extent of the visual adaptation field.

4.3 Contrast threshold measurements in high-dynamic background images

Contrast threshold measurements were conducted in dynamic non-uniform background luminances simulating real driving conditions by using the same experimental setup as in section 4.2. Detection threshold measurements refer to the question ‘Can a target be seen?’ and were applied in several studies in the development of mesopic photometry [26][30-31]. Night-time driving scenes may include dark objects as well as glare sources with high luminances. Thus, studies using non-uniform backgrounds with complex surroundings are needed. Previous studies indicate that the local luminance of the target is an essential factor in peripheral target detection in non-uniform backgrounds [9][27]. This supports the local adaptation [32] approach, which assumes that each part of the retina adjusts its light sensitivity independently.

A background image was taken in a street illuminated by LED luminaires (Figure 17). The S/P ratio of the background light is 2.02. The images were taken with Canon 60D camera combined with an 8 mm fish-eye lens located on the front of the car, between the headlamps. The luminaries and the car headlamps were on when images were taken.

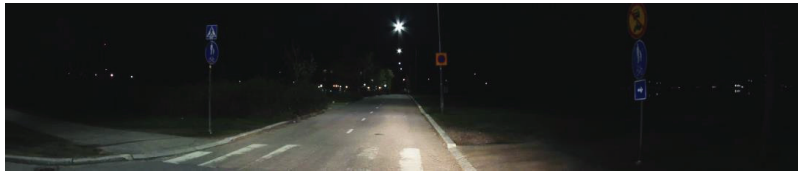


Figure 17. A background image taken from Otaranta in Espoo, Finland. The street is illuminated with LED luminaires.

Display devices such as screens and projectors have a non-linearity between RGB and luminance values called gamma. Gamma is the exponent in the power function:

$$S_{\text{out}} = AS_{\text{in}}^{\gamma} \quad (4)$$

where A is a scaling constant, S_{out} is the signal after gamma encoding, S_{in} is the signal to be encoded and γ is gamma. Gamma encoding is used to store luminance levels more efficiently. The gamma values of the projectors used were 2.2. In this experiment, the linearity between tristimulus and luminance is needed in order to control the increment of the target luminance and obtain its desired value. Thus, the inverse function to the gamma function was used to make the relation linear.

Targets with the size of 1.5° were projected onto the background in 23 different locations (Figure 18). Target locations cover 10° and 20° circular fields of view and include the horizontal eccentricities of -60° , -45° , -30° , 30° , 45° and 60° . There were two luminance levels for the background. Luminances of the background were adjusted by applying neutral density filters to obtain the average road surface luminance (1.6 cd/m^2 in a low luminance image; 3.4 cd/m^2 in a high luminance image), which is close to that measured from the street (1.8 cd/m^2), and the luminance of the luminaires was kept as high as possible considering the luminance range provided by the projectors (19 cd/m^2 in the low luminance image; 37 cd/m^2 in the high luminance image). Filters with 0.6 optical densities were used for high luminance images and filters with 0.9 optical densities were used for low luminance images. Luminance values were measured by an LMK spectrophotometer and an LMT 1009 luminance meter. Luminances from the 3° field surrounding the target location were recorded as a background luminance for the target. Target luminance was increased until it reached a value twice the amount of its background luminance. The subjects' task was to indicate if they detect the target or not. The term 'contrast' in this study refers to the ratio in equation 3 where L_b is the background luminance of the 3° field onto which the target is projected and L_t is the target luminance.

In order to quantify the luminance distribution of the surrounding area at each target location, the term 'complexity' was derived based on the following formula:

$$\text{Complexity} = 1 - L_{\min}/L_{\text{ave}} \quad (5)$$

where L_{\min} is the minimum luminance of the 5° field that surrounds each target location and L_{ave} is the average luminance of the same field.

Ten subjects (mean age: 30) participated in the experiment. All subjects had normal colour vision measured by the Ishihara colour vision test. The subjects were given 5 minutes to adapt to the background luminance before the experimental sessions. After adapting to the background, the subjects were asked to fixate on the cross at the centre of the screen binocularly and press the button when they detected the targets. An ascending method of limits was applied in the experiment. The target duration was 10 seconds. If no response was given by the subjects during this period it was recorded as a miss. The time between

target appearances (between 500 ms and 2000 ms) and the order of target locations were randomized. Exceptionally low contrast values ($< \text{mean} - 2 \times \text{standard deviation}$) were discarded from the results to eliminate anticipatory.

4.3.1 Results

There were two different luminance levels that are referred to as low and high luminance in this study. The luminance range of the low luminance image (shown with a neutral density filter with an optical density of 0.9) is between 0.05 and 19 cd/m^2 (the average luminance for the whole image was 0.34 cd/m^2). For the high luminance image (neutral density filter with an optical density of 0.6) the luminance values are between 0.1 and 37 cd/m^2 (the average luminance for the whole image was 0.76 cd/m^2). Target locations are indicated by numbers in Figure 18. The target number and the corresponding location in terms of horizontal and vertical eccentricities according to the fixation point (number 12 in Figure 18) are given in Table 5 in the appendices. The dots with numbers 7, 8, 9, 11, 13, 15, 16 and 17 represent the targets in the 10° field of view, whereas those with numbers 4, 5, 6, 10, 14, 18 and 19 refer to the targets in the 20° field of view. Other numbers correspond to the targets at horizontal eccentricities of -60° , -45° , -30° , 30° , 45° and 60° . The location of the targets with numbers 10 and 13 are shifted gradually so as not to overlap high-luminance objects in the scene.



Figure 18. Target locations illustrated with numbers in the background image of the road scene with LED luminaires. Number 12 is the fixation point.

According to the t-test there were no significant effects of the luminance level on the contrast threshold: $t(498) = -0.202$, $p = 0.840$. A two-way ANOVA was applied to check the effects of target location and target luminance on the contrast threshold values. The statistical analysis indicates that both target luminances ($F = 1.68$; $p < 0.03$) and target locations ($F = 11.99$; $p < 0.01$) had a significant effect on the contrast threshold. However, the interaction between them was not significant ($F = 0.83$; $p = 0.51$). A post-hoc Tukey test was applied to ascertain the effect of individual target locations. The contrast thresholds of the targets in the 10° and 20° fields of view with the same background luminance were close to each other. Target number 7 at a 10° eccentricity is one exception; target number 7 also had a higher contrast threshold at the higher luminance.

Mean contrast threshold values for the targets located on the horizontal axis (targets numbered 1, 2, 3, 4, 7, 12, 17, 20, 21, 22 and 23) at both luminance levels are shown in Figures 19 and 20. The figures indicate that visual sensitivity does

not depend on the target eccentricity but more on the local luminance and the complexity of the surrounding area. Another interesting and unexpected result is that the contrast threshold of the target at -10° (number 7) in the low luminance image is lower than that in the high luminance image. This target is surrounded by small bright spots that may make target detection more difficult in the high luminance image. Targets appeared on the right-hand side of the visual field (10° , 20° , 30° and 45°), which has less complex surroundings, were easier to detect. Far peripheral targets (-60° and 60°) were missed by most of the subjects as expected.

Contrast threshold values for targets within the 10° and 20° fields as a function of background luminance are presented in Figures 21 and 22 for both luminance levels. The figures indicate that targets appearing on the road surface were detected more easily (targets no. 5, 8, 10 and 11) at both luminance levels. However, targets that appeared at the edge of the pavement (nos. 15 and 18) were difficult to detect. Moreover, the contrast threshold for the target at 10° eccentricity (no. 17), which is located beside the pole with a traffic sign on it, is higher than that at 20° (no. 20), which has a more uniform surrounding. This indicates the effect of the complexity of the surrounding area on visual sensitivity in mesopic conditions.

However, Figures 21 and 22 indicate that targets number 4 (-20°) and 7 (-10°) have very high contrast threshold values, although there are other targets which have more complex surroundings in the same field of view (target no. 13 in the 10° field and target no. 14 in the 20° field). A similar result was observed for target number 17 in the 10° field. According to the numerical values obtained, we cannot attribute this fact to luminance distribution, local luminance or target location in a straightforward manner. However, it is proposed that the surroundings, including small bright spots and trees, make it more difficult to detect these targets, although this conclusion cannot be clearly verified based on their complexity values.

It was also difficult to detect a target (no. 14) appearing above the luminaire, which was the area with the highest luminance. High miss rates (Table 4) and contrast threshold values indicate that luminaires affect visual performance by causing disability glare.

According to Figures 19 and 20, the big difference in the contrast threshold values between targets 2 (-45°) and 3 (-30°), and targets 22 (45°) and 23 (60°) can be due to the traffic sign's pole being located between those targets. The contrast threshold difference between target number 2 at -45° eccentricity and target number 22 at 45° eccentricity also supports this hypothesis. These vertical objects may also make it difficult to detect targets in the far periphery (targets 2 and 23).

The foveal targets do not have the lowest contrast threshold values because their appearance was relatively unexpected for the subjects who had been giving responses to off-axis targets at several locations.

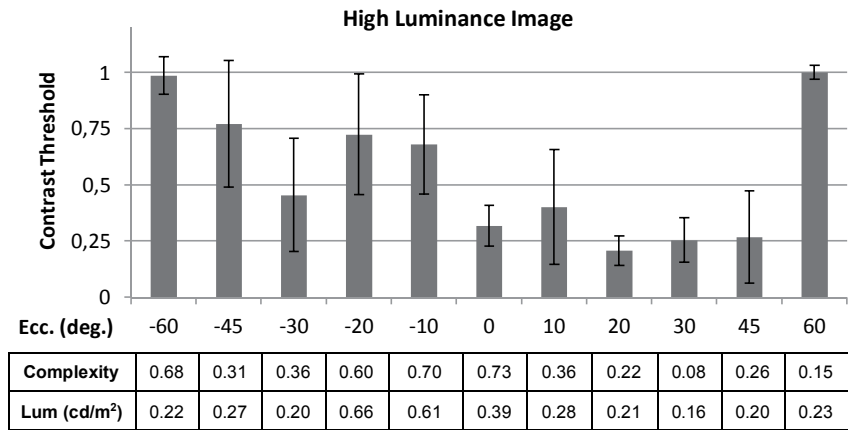


Figure 19. The contrast threshold of the targets on the horizontal axis in high luminance images as a function of eccentricity. The complexity of the 5° field and the background luminance at the corresponding target location are presented. Error bars indicate the standard deviation of the mean.

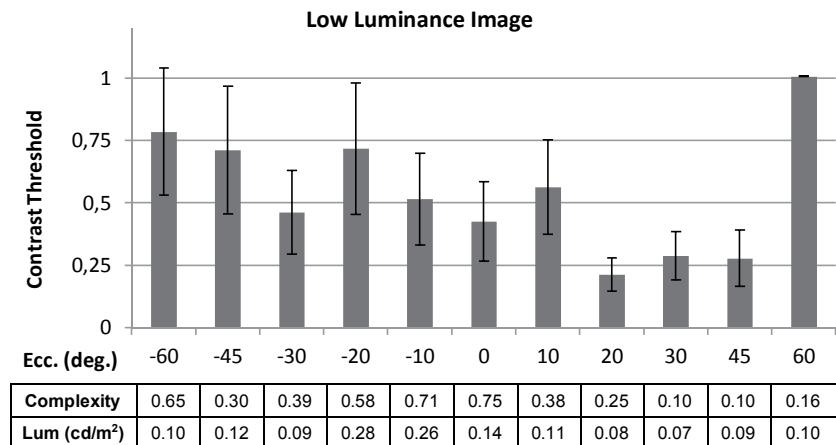


Figure 20. The contrast threshold of the targets on the horizontal axis in low luminance images as a function of eccentricity. The complexity of the 5° field and the background luminance at the corresponding target location are presented. Error bars indicate the standard deviation of the mean.

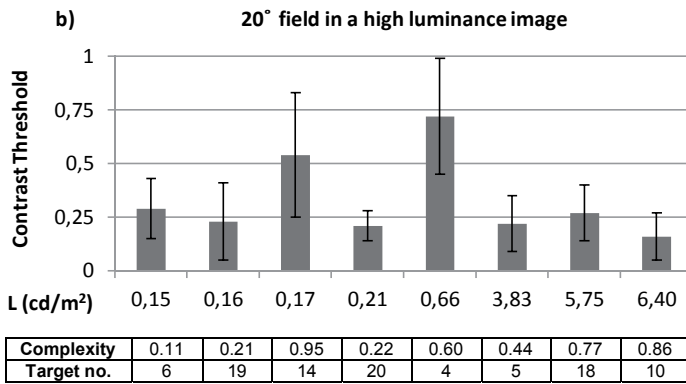
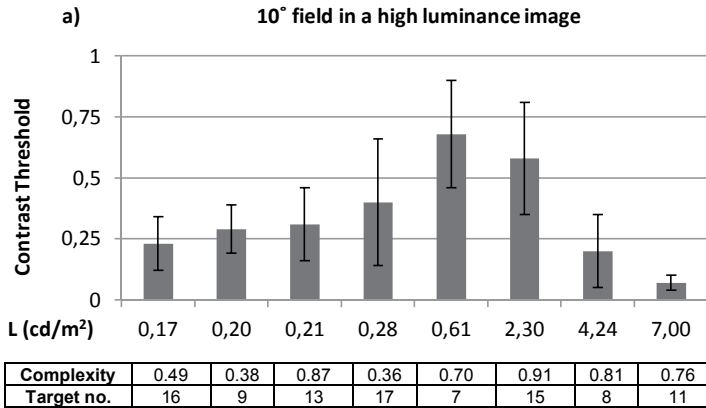
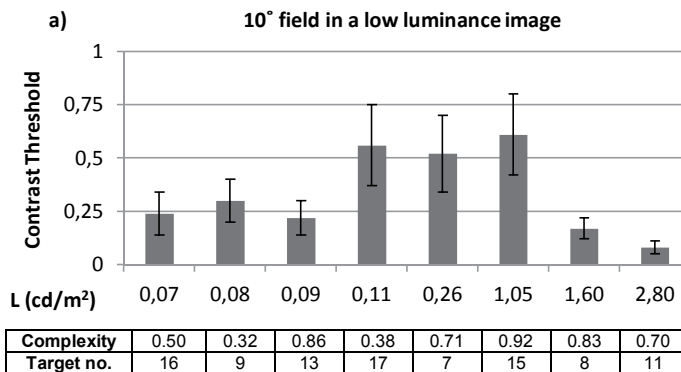
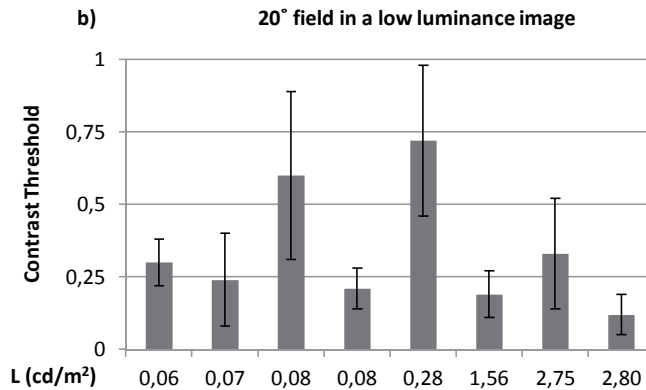


Figure 21. The contrast thresholds in high luminance images as a function of the background luminance of the targets in the (a) 10° and (b) 20° fields. The complexity of the 5° field at the corresponding target location and target number were presented below the horizontal axis. Error bars indicate the standard deviation of the mean.





Complexity	0,13	0,25	0,92	0,25	0,58	0,47	0,76	0,59
Target no.	6	19	14	20	4	5	18	10

Figure 22. The contrast thresholds in low luminance images as a function of the background luminance of the targets in the (a) 10° and (b) 20° fields. The complexity of the 5° field at the corresponding target location and target number were presented below the horizontal axis. Error bars indicate the standard deviation of the mean.

4.3.2 The effect of high luminance objects on peripheral target detection

Further contrast threshold measurements were carried out for a modified background image. The high luminance objects, such as street luminaires and other bright light spots, were removed in order to see their effect on peripheral target detection. The modified background is shown in Figure 23. The modified background image was named as ‘the image without luminaire luminances’ whereas the original background in Figure 18 is called ‘the image with luminaire luminances’ in this section. The luminance range of the low luminance image (neutral density filter with an optical density of 0.9) is between 0.04 and 6.9 cd/m² (the average luminance for the whole image was 0.27 cd/m²). For the high luminance image (neutral density filter with an optical density of 0.6) the luminance values are between 0.08 and 17 cd/m² (the average luminance for the whole image was 0.57 cd/m²).

Target number and the corresponding location in terms of horizontal and vertical eccentricities according to the fixation point (number 12 in Figure 23) are given in Table 6 in the Appendices. The contrast thresholds for targets appearing in the horizontal axis for low and high luminance images are shown in Figure 24.



Figure 23. Background image without any luminaire and other light spots. Target locations are shown by numbers.

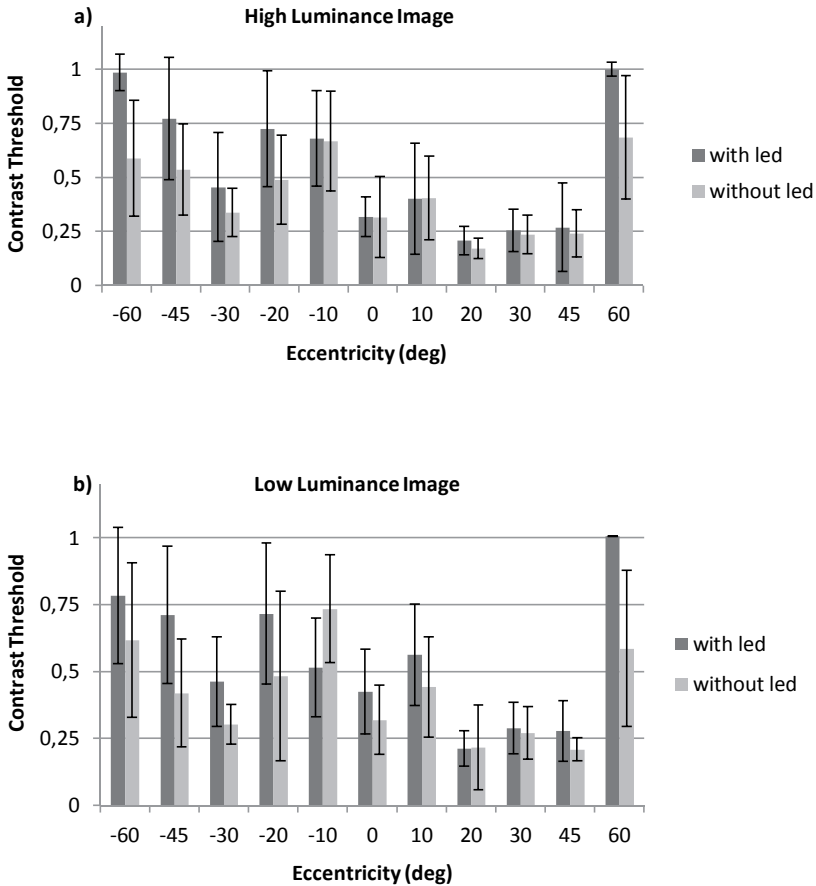


Figure 24. The contrast threshold of the targets on the horizontal axis in high (a) and low (b) luminance images without the luminaire as a function of eccentricity

In the low luminance image, no differences were found in contrast thresholds between the images with change and without change for the targets at 20° and 30° eccentricities (nos. 21 and 22). However, lower contrast thresholds were obtained for the targets at 60°, 10°, -20°, -30°, -45°, -60° in the background image without luminaires than in the image with luminaires (Fig. 24). For target number 7 at -10°, the contrast threshold is high relative to those for targets at

other locations in the 10° field of view due to the luminance distribution of the target surroundings. Target number 7 is surrounded by light spots and small trees that look more complex compared to target number 17 which is located at its symmetry. However, the contrast threshold for that target becomes higher in the background with no luminaire. This cannot be attributed to low local luminance alone (which is 0.12 cd/m^2) since target number 4 at -20° has the same background luminance.

There were almost no differences in the contrast thresholds between backgrounds with luminaires and without luminaires in the high luminance images for targets at 20° , 30° and 45° (nos. 20, 21 and 22) (Figure 24a). Also, the mean contrast threshold values are almost the same at -10° , 0° and 10° eccentricities. However, as with low luminance background images, the contrast thresholds were lower at eccentricities 60° , 10° , -20° , -30° , -45° and -60° in the background image without luminaires (Figure 24b).

There were no differences in the contrast threshold between the targets with uniform luminance surroundings in the 10° and 20° circular fields of view. However, at low background luminances, contrast thresholds decrease for targets at 0° and 10° eccentricities (nos. 12 and 17) when luminaires and other light spots were removed, contrary to results with high luminance background images. This can be attributed to higher visual sensitivity at lower adaptation luminances.

It is difficult to detect the target located beside the closest luminaire in the 20° field of view (number 14). The effect of removing the luminaire from the background can be seen for that target clearly. The rate of missed targets in that location is also high (Table 5) relative to the other targets in the near periphery (10° and 20° eccentricities). After removing the luminaire from the background, luminance distribution becomes uniform, the contrast threshold decreased and the rate of missed targets became zero. There is another target located near the luminaire in the 20° field of view (number 13). However, the effect of removing luminaires in that location can only be seen with the high luminance background.

Removing the high luminance objects from the background image in this study did not affect the road surface luminances. However, it affects the contrast thresholds for targets, mostly in the far periphery (-60° , -45° , 45° and 60°). Statistical analysis also indicates that the effect of high luminance objects is significant on peripheral target detection ($t(998) = -5.04$; $p = 0.00$).

4.3.3 Discussion

The control of the luminance and the location of the targets make laboratory experiments more useful than field experiments. However, simulations of night-time driving do not provide a high enough luminance range for real night-

time driving conditions. Correspondingly, the experimental set-up was restricted to stationary images taken from the road.

It was found that the luminance of the target according to its location (local luminance) affects visual sensitivity, as expected. However, applying a night-time driving image as the background indicates that the luminance distribution of the area surrounding the targets also plays an essential role in peripheral target detection rather than target eccentricity.

The contrast thresholds were lower for targets at the right periphery (20° , 30° and 45°) compared to those at same eccentricities at the left periphery since the luminance distribution of the background at the right periphery was uniform. On the other hand, surrounding areas of the target locations at the left periphery include trees in both backgrounds and small bright spots in the background with luminaires. This indicates that luminance distribution of the immediate background affects the detection of targets in peripheral vision. Targets at the left periphery have lower contrast thresholds in the background with no luminaires.

The luminance of the luminaire (in high luminance images) was 37 cd/m^2 , which was quite low compared to real conditions. The luminance of that particular luminaire under real conditions would be more than 1000 cd/m^2 , which the projectors used in the set-up could not possibly provide. Although the difference is extremely large, it was still possible to determine that it is difficult to detect targets close to bright objects that cause disability glare. The missing rate was higher for the target located above the luminaire, shown as number 14 in Figure 18. It is assumed that the visual adaptation field will be affected by the location of the glare source as well. The luminance level of the background was adjusted by applying neutral density filters. However, the effect of the average luminance of the background on the contrast threshold was not statistically significant.

The contrast thresholds for targets in a 10° field of view were quite close to the values obtained for the targets in a 20° field of view with the same background luminance when excluding the targets surrounded by a more complex field. Visual sensitivity was also higher for targets with more uniform surroundings at 30° and 45° eccentricities at both luminances.

The effect of the average luminance of the background on the contrast detection threshold was not significant based on the statistical analysis. Therefore, it is not possible to comment on the extent to which the adaptation luminance level affected the contrast detection threshold for a specific target location in the high and low luminance images. However, if targets in the same field of view are considered, an effect of the target background luminance on contrast detection threshold was found. A lower contrast detection threshold for the targets in the 10° and 20° fields of view along the road's surface compared to targets not on the road can be attributed to the local adaptation mechanism of the retina. Similar contrast detection threshold values for targets with the same local background luminance in the 10° and 20° fields of view (target numbers 6 and 9, 5 and 8, 16 and 19) can also be attributed to the local adaptation effect. However, contrast threshold values at -45° , -30° , -20° , -10° and 10° , which depend on the

complexity of the surrounding area of the targets, can be attributed to a cognitive mechanism which could make the target detection difficult even if the adaptation level is same. The effect of the area surrounding the road on the contrast detection threshold should be attributed to a cognitive mechanism rather than to the adaptation level.

In night-time driving conditions, defining the background luminance is not a straightforward process since the visual fields are complex and have various luminances. It will be more difficult to analyse background luminances in a moving scene where the presence and the effect of the objects change as the car moves rather than appearing as a static image, as they did in the experiments. In driving, objects are not static relative to the driver, in contrast to those in the backgrounds applied in these experiments. However, the area surrounding the road under real driving conditions, such as the flow of trees, buildings and signs, may have a similar effect on the extent of the visual field. An increase in the complexity of the background reduces a subject's ability to detect targets. Therefore, the extent of the visual field also depends on the area surrounding the road.

5. Conclusions

The CIE system of mesopic photometry [2] includes methods for defining spectral sensitivity and mesopic luminance between luminances from 0.005 cd/m^2 to 5 cd/m^2 . Defining the visual adaptation field in terms of its extent and shape is an important goal in order to implement this system in outdoor lighting.

The Illuminating Engineering Society (IES) released a memorandum 'IES TM-12-12' in 2012 [42]. In this publication adaptation luminance is defined as 'the average luminance of the field of view, or in the case of local adaptation, of a particular portion of the field of view'. 'A particular portion of the field of view' in this definition refers to the term 'visual adaptation field'. Adaptation luminance defines the response of the visual system to the objects in the field of view. As adaptation luminance increases, the contrast threshold decreases, resulting in increased visual performance.

Boyce [3] states that the usual way of describing the state of adaptation is by evaluating the luminance of the visual field to which the observer is adapted. This is straightforward under laboratory conditions where the visual field can be adjusted to be uniform. In this case, adaptation luminance can be considered as the luminance of the uniform background. However, in real driving conditions, the situation is different as the luminance values and luminance distribution of the visual field are constantly changing. There is no clear method to estimate adaptation luminance when the luminance of the visual field is non-uniform and the gaze direction of the driver is constantly changing. In this study, both field and laboratory measurements were done to develop methods for estimating the field of view of which the luminance is to be used as the adaptation luminance.

In the study of combining eye-tracking measurements with luminance data, the visual scene areas with the highest density of gaze distributions were determined. The measured luminances for these visual scenes were used to form an estimate of the adaptation luminance under different driving conditions in the lit and the unlit sections of a rural road. The mean luminances of the estimated fields were higher in the unlit section than in the lit section of the route for all drivers. This was due to high-beam headlights that illuminated the road surface, and the gaze points were concentrated on the unlit section. Moreover, variations in the mean luminance as a function of distance diminished as the size of the circular visual field increased.

Experiments in laboratory conditions where it is possible to control background luminance were conducted in order to obtain the effect of background luminance distribution and target location and target luminance on visual performance. Reaction time and contrast threshold measurements were made to analyse peripheral target detection in uniform and non-uniform luminous backgrounds. Under non-uniform background luminances peripheral target detection depends on the local luminance of the target and the luminance uniformity of the surrounding area of the target. The results verify that each part of the retina adjusts its sensitivity independently, which refers to local adaptation. However, the complexity of the visual field also has an effect on visual sensitivity in peripheral vision.

The visual adaptation field is expected to be affected by the surroundings of the road in terms of both the luminance distribution and the objects and buildings located in them. Further studies where road type, driving speed and discomfort glare are taken into account are needed to define the visual adaptation field and corresponding adaptation luminance in various driving conditions.

6. References

1. Puolakka M., Cengiz C., Luo W., Halonen L. 'Implementation of CIE 191 Mesopic Photometry – Ongoing and Future Actions'. Proceedings CIE 2012 Lighting Quality and Energy Efficiency. Hangzhou, China, Sep 19–21: 2012: 64–70.
2. Commission Internationale de l'Eclairage. 'Recommended System for Mesopic Photometry Based on Visual Performance'. CIE Publication 191-2010, Vienna: CIE, 2010.
3. Boyce P. R. Human Factors in Lighting. CRC Press: Taylor and Francis Group, 2014.
4. M. Ikeda and H. Shimozone. 'Mesopic luminous-efficiency functions'. Journal of the Optical Society of America A: Optics, image science, and vision, vol. 71, no. 3, pp. 280–284, Mar. 1981.
5. K. Sagawa and K. Takeichi. 'Spectral luminous efficiency functions in the mesopic range'. Journal of the Optical Society of America A: Optics, image science, and vision, vol. 3, no. 1, pp. 71–75, Jan 1986.
6. D. Schreuder. 'Outdoor Lighting: Physics, Vision and Perception'. Springer Science Business Media B. V., 2008.
7. Commission Internationale de L'Eclairage. 'International Lighting Vocabulary'. CIE S 017/E: 2011. ILV. Vienna: CIE, 2011.
8. J. N. ver Hoeve. 'Visual Adaptation'. Retrieved December 2014. Available at: <http://www.oculist.net/downat0502/prof/ebook/duanes/pages/v8/v8c016.html#ref>
9. Uchida T, Ohno Y. 'Defining visual adaptation field for mesopic photometry: Does surrounding luminance affect peripheral adaptation?' Lighting Research and Technology, vol. 46, pp. 520–533, 2014.
10. Narisada K. 'Visual Perception in Non-uniform Fields'. Journal of Light and Visual Environment, vol. 16, no.2, pp. 83-88, 1992.
11. S. Plainis, I. J. Murray and W. N. Charman. 'The Role of Retinal Adaptation in Night Driving'. Optometry and Vision Science, vol. 82, no. 8, pp. 682–88, Aug. 2010.
12. B. M. Matesanz, L. Issolio, I. Arranz, C. de la Rosa, J. A. Menedez, S. Mar and J. A. Aparico. 'Temporal retinal sensitivity in mesopic adaptation'. Ophthalmic & Physiological Optics: The Journal of the British College of Ophthalmic Opticians (Optometrists), vol. 31, no. 6, pp. 615–624, Nov. 2011.
13. J. W. A. M. Alferdinck, M. A. Hogervorst, A. M. J. van Eijk and J. T. Kusmierczyk. 'Mesopic vision and public lighting – A literature review and a face recognition experiment'. TNO-DV 2010 C435, TNO Defence, Security and Safety, Soesterberg, The Netherlands, December 2010.

14. Mourant R. R., Rockwell T. H. 'Strategies of visual search by novice and experienced drivers'. *Human Factors*, vol. 14, pp. 325–335, 1972.
15. Falkmer T., Gregersen N. P. 'A comparison of eye movement behaviour of inexperienced and experienced drivers in real traffic environments'. *Optometry and Vision Science*, vol. 82, pp. 732–739, 2005.
16. Maltz M., Shinar D. 'Eye movements of younger and older drivers'. *Human Factors*, vol. 41, pp. 15–25, 1999.
17. Land M. F. 'Predictable eye-head coordination during driving'. *Nature*, vol. 359, pp. 318–319, 1992.
18. Land M. F., Lee D. 'Where we look when we steer'. *Nature*, vol. 369, pp. 742–744, 1994.
19. Kandil F. I., Rotter A., Lappe M. 'Car drivers attend to different gaze targets when negotiating closed vs. open bends'. *Journal of Vision*, 2010, vol. 10, April, 2010.
20. Lappi O., Lehtonen E. 'Eye-movements in real curve driving: Pursuit-like optokinesis in vehicle frame of reference, stability in an allocentric reference coordinate system'. *Journal of Eye Movement Research*, vol. 6, pp. 1–13, 2013.
21. Lehtonen E., Lappi O., Kotkanen H., Summala H. 'Look-ahead fixations in curve driving'. *Ergonomics*, vol. 56, pp. 34–44, 2013.
22. Tiehallinto. 'Tievalaistuksen suunnittelu'. Edita Prima Oy. Retrieved December 2012. Available at: http://alk.tiehallinto.fi/thohje/pdf/2100034-v-06tievalaist_suunn.pdf.
23. Rea M. S. 'The Trotter Paterson Lecture 2012: Whatever happened to visual performance?' *Lighting Research Technology*, vol. 44, pp. 95–108, 2012.
24. Plainis S., Murray J. 'Reaction times as an index of visual conspicuity when driving at night'. *Ophthalmic and Physiological Optics*, vol. 22, pp. 409–415, 2002.
25. Walkey H., Orrevelainen P., Barbur J., Halonen L., Goodman T., Alferdinck J., Freiding A., Szalmas A. 'Mesopic visual efficiency II: reaction time experiments'. *Lighting Research and Technology*, vol. 39, pp. 335–354, 2007.
26. Eloholma M., Ketomaki J., Orrevelainen P., Halonen L. 'Visual performance in night-time driving conditions'. *Ophthalmic and Physiological Optics*, vol. 26, pp. 254–263, 2006.
27. Akashi Y., Rea M. S., Bullough J. D. 'Driver decision making in response to peripheral moving targets under mesopic light levels'. *Lighting Research and Technology*, vol. 39, pp. 53–67, 2007.
28. Webster M. A., MacLeod D. I. A. 'Visual adaptation and face perception'. *Philosophical Transactions of the Royal Society: Biological Sciences*, vol. 366, pp. 1702–1725, 2011.
29. Rieke F., Rudd M. E. 'The challenges natural images pose for visual adaptation'. *Neuron*, vol. 64, pp. 605–616, 2009.
30. Walkey H. C., Harlow J. A., Barbur J. L. 'Characterising mesopic spectral sensitivity from reaction times'. *Vision Research*, vol. 46, pp. 4232–4243, 2006.

31. Raphael S., Leibenger M. 'Models of mesopic photometry applied to the contrast threshold of peripheral and foveal objects'. Proceedings of the 26th Session of the CIE, Beijing, 2007.
32. Illuminating Engineering Society of North America. 'Spectral Effects of Lighting on Visual Performance at Mesopic Lighting Levels'. IES TM-12-12. New York, NY: IESNA, 2012.

7. Appendices

Table 5. The mean value of the contrast threshold (CT) values for the targets for (a) low and (b) high luminance levels with their numbers (no.) based on Figure 18 and corresponding locations in terms of horizontal (h) and vertical (v) eccentricities. L_p is the photopic luminance and L_{mes} is the mesopic luminance of the 3° field of view wherein the target was imposed. Std. is the standard deviation for the mean value of contrast thresholds. Comp. is the 'complexity of the 5° field that surrounds the target location'. Miss is the percentage of missed targets.

no.	h (deg)	v (deg)	Low luminance image					
			L_p (cd/m^2)	L_{mes} (cd/m^2)	CT	std.	comp.	miss (%)
1	-60	0	0.1	0.13	0.79	0.25	0.65	48.15
2	-45	0	0.12	0.16	0.71	0.26	0.30	25.93
3	-30	0	0.09	0.12	0.46	0.17	0.39	0
4	-20	0	0.28	0.34	0.72	0.26	0.58	33.33
5	-12	-16	1.56	1.67	0.19	0.08	0.47	0
6	-12	16	0.06	0.08	0.3	0.08	0.13	0
7	-10	0	0.26	0.32	0.52	0.18	0.71	0
8	-6	-8	1.6	1.7	0.17	0.05	0.83	0
9	-6	8	0.08	0.11	0.3	0.1	0.32	0
10	-2	-20	2.8	2.9	0.12	0.07	0.59	0
11	0	-10	2.8	2.9	0.08	0.03	0.70	0
12	0	0	0.14	0.18	0.43	0.16	0.75	3.45
13	1	10	0.09	0.12	0.22	0.08	0.86	0
14	0	20	0.08	0.11	0.6	0.29	0.92	25
15	6	-8	1.05	1.15	0.61	0.19	0.92	3.85
16	6	8	0.07	0.1	0.24	0.1	0.50	0
17	10	0	0.11	0.14	0.56	0.19	0.38	0
18	12	-16	2.75	2.85	0.33	0.19	0.76	16.67
19	12	16	0.07	0.1	0.24	0.16	0.25	0
20	20	0	0.08	0.11	0.21	0.07	0.25	0
21	30	0	0.07	0.1	0.29	0.1	0.10	0
22	45	0	0.09	0.12	0.28	0.11	0.10	0
23	60	0	0.1	0.13	1.01	0	0.16	96.15

(a)

		High Luminance Image						
no.	h (deg)	v (deg)	L _p (cd/m ²)	L _{mes} (cd/m ²)	CT	std.	comp.	miss (%)
1	-60	0	0.22	0.27	0.99	0.08	0.68	87.5
2	-45	0	0.27	0.33	0.77	0.28	0.31	46.2
3	-30	0	0.2	0.25	0.46	0.25	0.36	7.4
4	-20	0	0.66	0.75	0.72	0.27	0.60	33.3
5	-12	-16	3.83	3.89	0.22	0.13	0.44	0
6	-12	16	0.15	0.19	0.29	0.14	0.11	0
7	-10	0	0.61	0.7	0.68	0.22	0.70	13.3
8	-6	-8	4.24	4.28	0.2	0.15	0.81	0
9	-6	8	0.2	0.25	0.29	0.1	0.38	0
10	-2	-20	6.4	6.4	0.16	0.11	0.86	23.8
11	0	-10	7	7	0.07	0.03	0.76	0
12	0	0	0.39	0.46	0.32	0.09	0.73	0
13	1	10	0.21	0.26	0.31	0.15	0.87	0
14	0	20	0.17	0.21	0.54	0.29	0.95	24.1
15	6	-8	2.3	2.41	0.58	0.23	0.91	3.6
16	6	8	0.17	0.21	0.23	0.11	0.49	0
17	10	0	0.28	0.34	0.4	0.26	0.36	0
18	12	-16	5.75	5.75	0.27	0.13	0.77	42.9
19	12	16	0.16	0.2	0.23	0.18	0.21	0
20	20	0	0.21	0.26	0.21	0.07	0.22	0
21	30	0	0.16	0.2	0.25	0.1	0.08	0
22	45	0	0.2	0.25	0.27	0.2	0.26	3.6
23	60	0	0.23	0.28	1	0.03	0.15	96.2

(b)

Table 6. The mean value of the contrast threshold values (CT) in (a) low and (b) high luminance conditions for the targets in the road scene with and without LED luminaires with their numbers (no.) based on Figure 23. Corresponding locations are indicated in terms of horizontal (h) and vertical (v) eccentricities. L is the luminance of the 3° field of view wherein the 1.5° target was imposed. Std. is the standard deviation for the mean value of contrast thresholds. Miss is the percentage of the missed targets.

Low luminance			With LED				Without LED			
no.	h (deg.)	v (deg.)	L (cd/m ²)	CT	std.	miss (%)	L (cd/m ²)	CT	std.	miss (%)
1	-60	0	0.1	0.79	0.25	48.15	0.09	0.62	0.29	24.14
2	-45	0	0.12	0.71	0.26	25.93	0.12	0.42	0.20	0.00
3	-30	0	0.09	0.46	0.17	0.00	0.08	0.30	0.07	0.00
4	-20	0	0.28	0.72	0.26	33.33	0.12	0.48	0.32	3.33
5	-12	-16	1.56	0.19	0.08	0.00	1.3	0.17	0.06	0.00
6	-12	16	0.06	0.30	0.08	0.00	0.06	0.26	0.09	0.00
7	-10	0	0.26	0.52	0.18	0.00	0.12	0.73	0.20	14.29
8	-6	-8	1.6	0.17	0.05	0.00	1.3	0.19	0.07	0.00
9	-6	8	0.08	0.30	0.10	0.00	0.07	0.27	0.12	0.00
10	-2	-20	2.8	0.12	0.07	0.00	2.4	0.09	0.05	0.00
11	0	-10	2.8	0.08	0.03	0.00	2.7	0.06	0.01	0.00
12	0	0	0.14	0.43	0.16	3.45	0.11	0.32	0.13	0.00
13	1	10	0.09	0.22	0.08	0.00	0.08	0.22	0.08	0.00
14	0	20	0.08	0.60	0.29	25.00	0.06	0.39	0.35	6.67
15	6	-8	1.05	0.61	0.19	3.85	0.93	0.41	0.14	0.00
16	6	8	0.07	0.24	0.10	0.00	0.06	0.21	0.06	0.00
17	10	0	0.11	0.56	0.19	0.00	0.1	0.44	0.19	0.00
18	12	-16	2.75	0.33	0.19	16.67	2.24	0.14	0.11	3.33
19	12	16	0.07	0.24	0.16	0.00	0.07	0.17	0.07	0.00
20	20	0	0.08	0.21	0.07	0.00	0.07	0.22	0.16	0.00
21	30	0	0.07	0.29	0.10	0.00	0.06	0.27	0.10	0.00
22	45	0	0.09	0.28	0.11	0.00	0.08	0.21	0.04	0.00
23	60	0	0.1	1.01	0.00	100.00	0.09	0.59	0.29	23.33

(a)

High luminance			With LED				Without LED			
no.	h (deg.)	v (deg.)	L (cd/m2)	CT	std.	miss (%)	L (cd/m2)	CT	std.	miss (%)
1	-60	0	0.22	0.99	0.08	87.5	0.18	0.59	0.27	20.00
2	-45	0	0.27	0.77	0.28	46.2	0.24	0.54	0.21	6.67
3	-30	0	0.2	0.46	0.25	7.4	0.17	0.34	0.11	0.00
4	-20	0	0.66	0.72	0.27	33.3	0.26	0.49	0.21	3.33
5	-12	-16	3.83	0.22	0.13	0.0	3.34	0.18	0.08	0.00
6	-12	16	0.15	0.29	0.14	0.0	0.13	0.23	0.07	0.00
7	-10	0	0.61	0.68	0.22	13.3	0.26	0.67	0.23	3.33
8	-6	-8	4.24	0.20	0.15	0.0	3.2	0.17	0.05	0.00
9	-6	8	0.2	0.29	0.10	0.0	0.18	0.23	0.09	0.00
10	-2	-20	6.4	0.16	0.11	23.8	6.12	0.09	0.05	0.00
11	0	-10	7	0.07	0.03	0.0	6.32	0.07	0.02	0.00
12	0	0	0.39	0.32	0.09	0.0	0.26	0.32	0.19	0.00
13	1	10	0.21	0.31	0.15	0.0	0.19	0.22	0.08	0.00
14	0	20	0.17	0.54	0.29	24.1	0.14	0.31	0.12	0.00
15	6	-8	2.3	0.58	0.23	3.6	2.11	0.41	0.15	0.00
16	6	8	0.17	0.23	0.11	0.0	0.15	0.19	0.09	0.00
17	10	0	0.28	0.40	0.26	0.0	0.22	0.40	0.19	3.33
18	12	-16	5.75	0.27	0.13	42.9	5.36	0.16	0.09	0.00
19	12	16	0.16	0.23	0.18	0.0	0.15	0.17	0.07	0.00
20	20	0	0.21	0.21	0.07	0.0	0.19	0.17	0.05	0.00
21	30	0	0.16	0.25	0.10	0.0	0.14	0.24	0.09	0.00
22	45	0	0.2	0.27	0.20	3.6	0.18	0.24	0.11	0.00
23	60	0	0.23	1.00	0.03	96.2	0.19	0.69	0.29	33.33

(b)

The aim of the study is to develop methods for estimating the field of view of which the luminance is to be used as the adaptation luminance in implementing the CIE 191 system for mesopic photometry. This is realised by applying methods such as combining eye-tracking data with corresponding luminance data and analysing peripheral target detection under uniform and non-uniform luminous backgrounds. In the study of combining eye-tracking measurements with luminance data, the visual scene areas with the highest density of gaze distributions were determined. Experiments in laboratory conditions were conducted in order to obtain the effect of background and target location and its luminance on visual performance. The results verify that each part of the retina adjusts its sensitivity independently, which refers to local adaptation. However, the complexity of the visual field also has an effect on visual sensitivity in peripheral vision.



ISBN 978-952-60-6439-0 (printed)

ISBN 978-952-60-6440-6 (pdf)

ISSN-L 1799-4934

ISSN 1799-4934 (printed)

ISSN 1799-4942 (pdf)

Aalto University
School of Electrical Engineering
Department of Electrical Engineering and Automation
www.aalto.fi

**BUSINESS +
ECONOMY**

**ART +
DESIGN +
ARCHITECTURE**

**SCIENCE +
TECHNOLOGY**

CROSSOVER

**DOCTORAL
DISSERTATIONS**